

Attachement to Doctoral Thesis

Robust Monitoring Procedures for Dependent Data

Ondřej Chochola

This document contains additional results of the simulation study as described in Chapter 6 of the thesis. Structure of the document is the same as that of Chapter 6. All figures relating to a specific figure of the thesis are grouped into one subsection. We do not comment the results as this is already done in the thesis.

1 Location Model

1.1 Figure 6.1

Following figures are analogues of Figure 6.1 (which is presented first), i.e. SPC for different LRV estimators under H_0 , where we vary types of procedures, tuning constants γ as well as types of dependence (AR(1) or MA(1)) and the distributions of innovations.

The color and line coding is the same in all figures, i.e.

Λ_m : 4 - black, 8 - red, 10- yellow, 20 - green, 40 - blue and accordingly for FLT adapt;
 m : 80 - dotted, 200 - dashed, 400 - solid.

Only the varying parameters are indicated in captions. We present 3 figures with $\gamma = 0, 0.25$ and 0.45 for each type. Firstly Huber procedure with AR(1) of $N(0, 1)$ innovations, then with Laplace innovations and t_3 innovations. Then the errors form MA(1) of $N(0, 1)$ innovations. Finally we show L_1 and L_2 procedures with errors forming AR(1) of $N(0, 1)$.

Huber_025

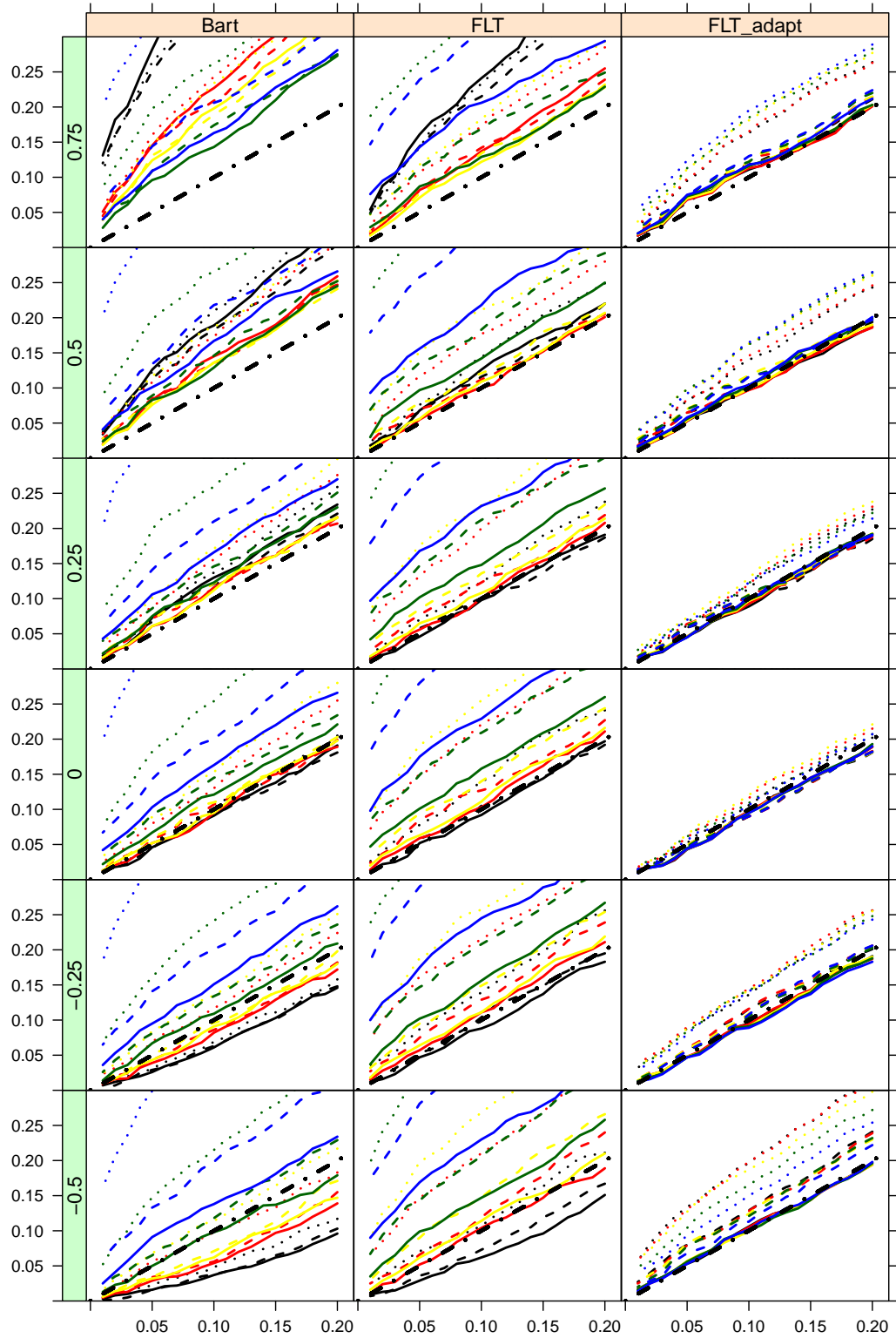


Figure 1: SPC for different LRV estimators, Huber procedure under H_0 , $\gamma = 0.25$, errors being AR(1) of $N(0, 1)$ innovations with ρ indicated at LHS of each panel.
 Λ_m : 4 - black, 8 - red, 10 - yellow, 20 - green, 40 - blue and accordingly for FLT adapt;
 m : 80 - dotted, 200 - dashed, 400 - solid.

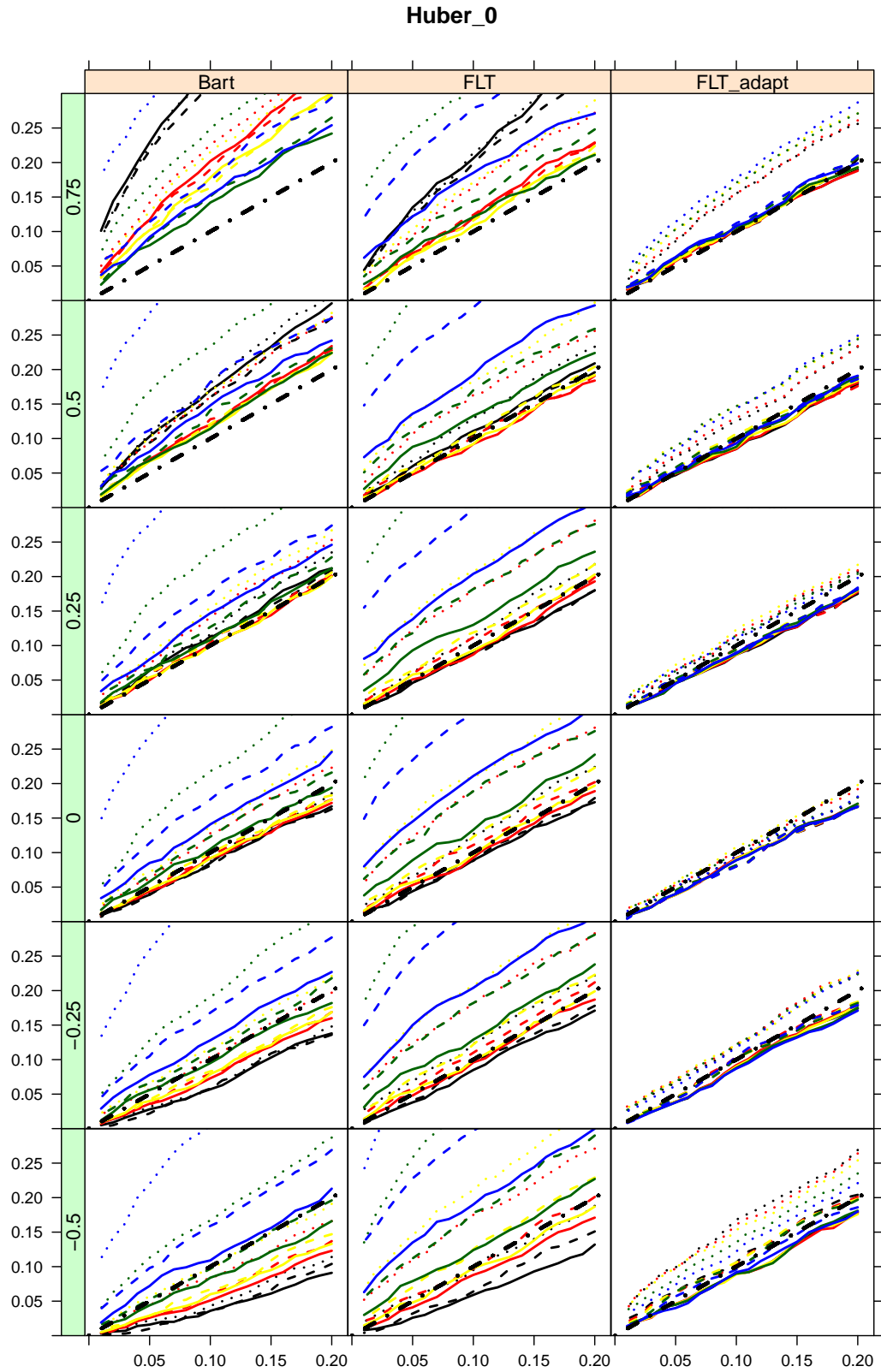


Figure 2: Huber procedure, $\gamma = 0$, errors being AR(1) of $N(0, 1)$ innovations with ρ indicated at LHS of each panel.

Huber_045

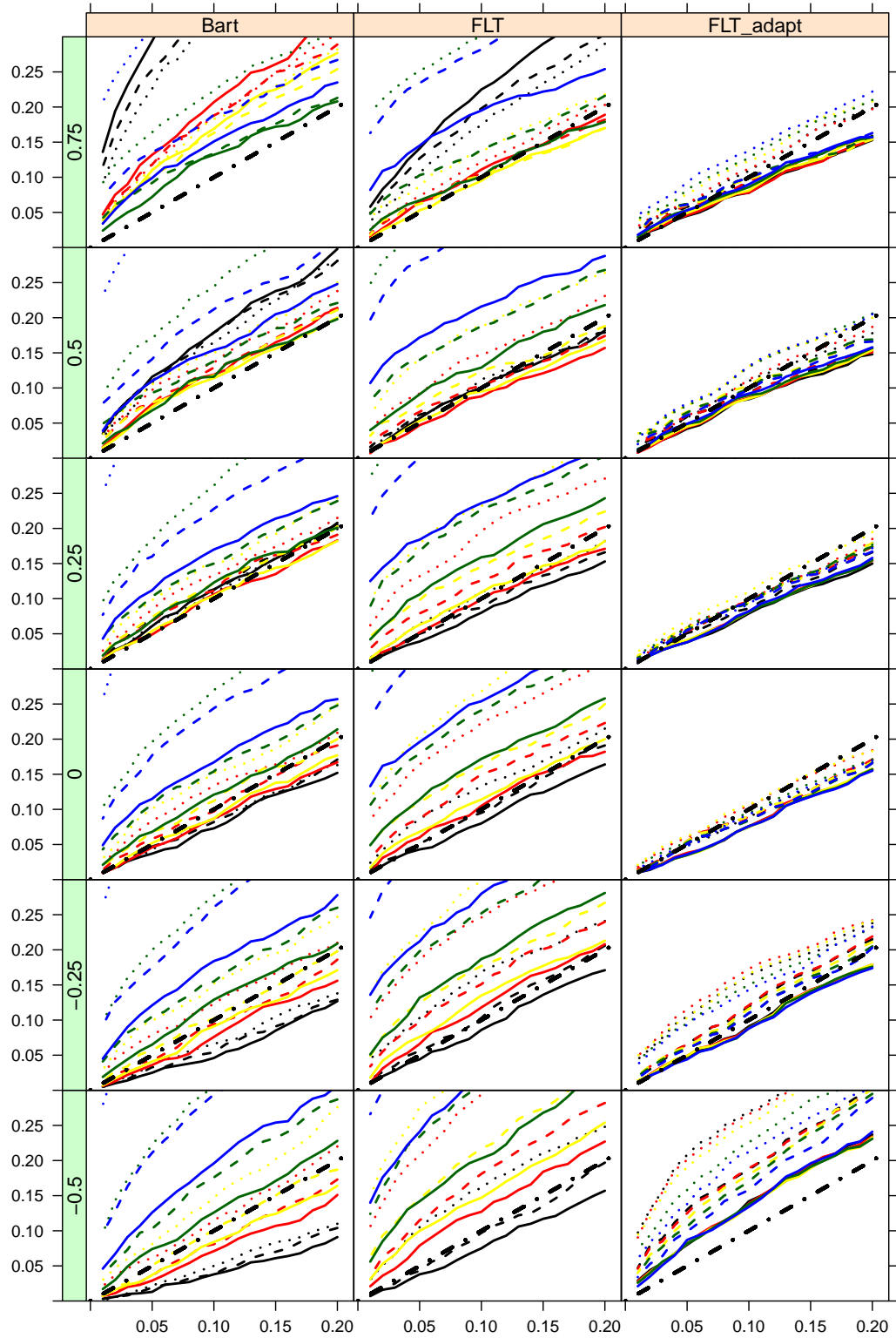


Figure 3: Huber procedure, $\gamma = 0.45$, errors being AR(1) of $N(0, 1)$ innovations with ρ indicated at LHS of each panel.

Huber_Lapl_0

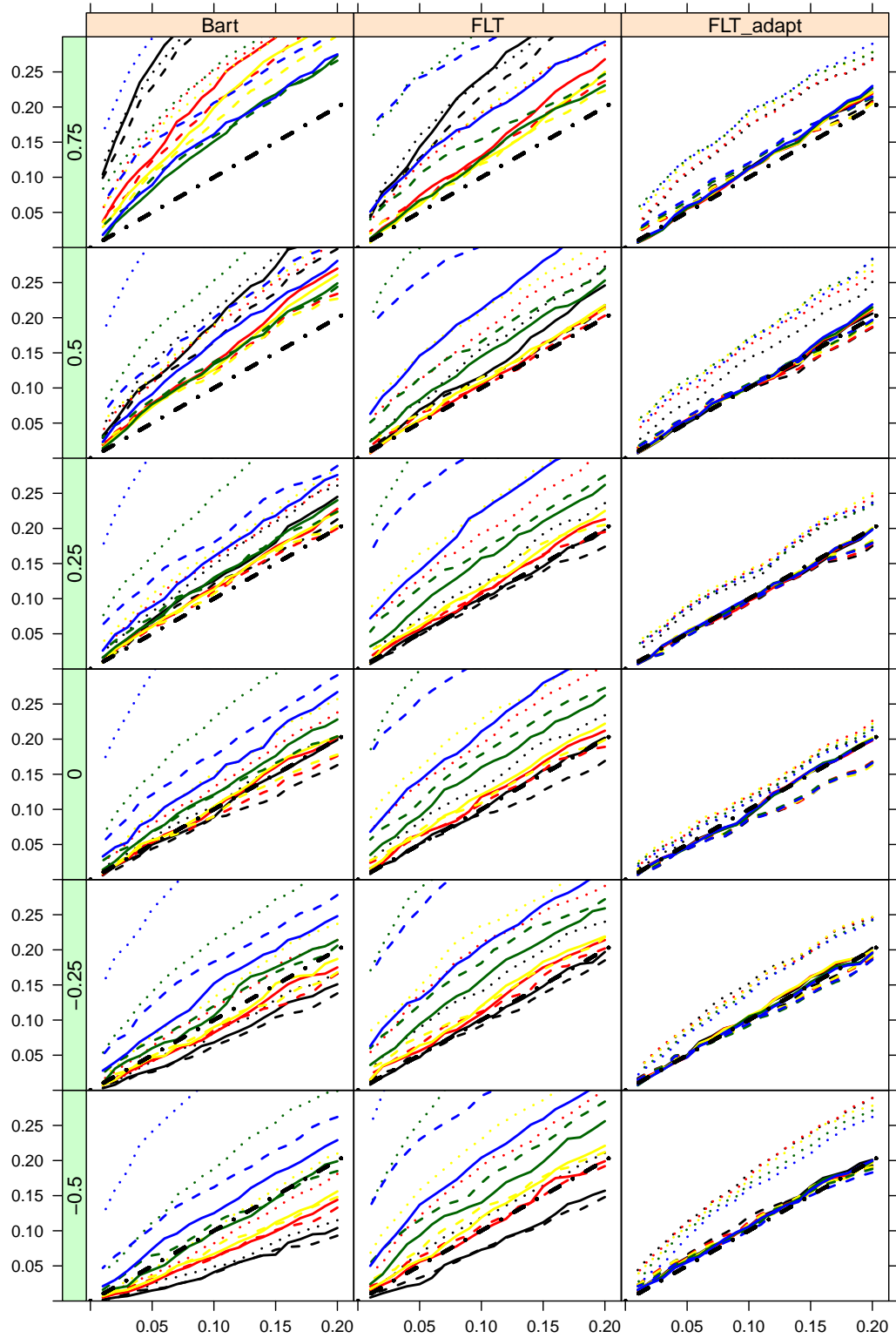


Figure 4: Huber procedure, $\gamma = 0$, errors being AR(1) of Laplace innovations with ρ indicated at LHS of each panel.

Huber_Lapl_025

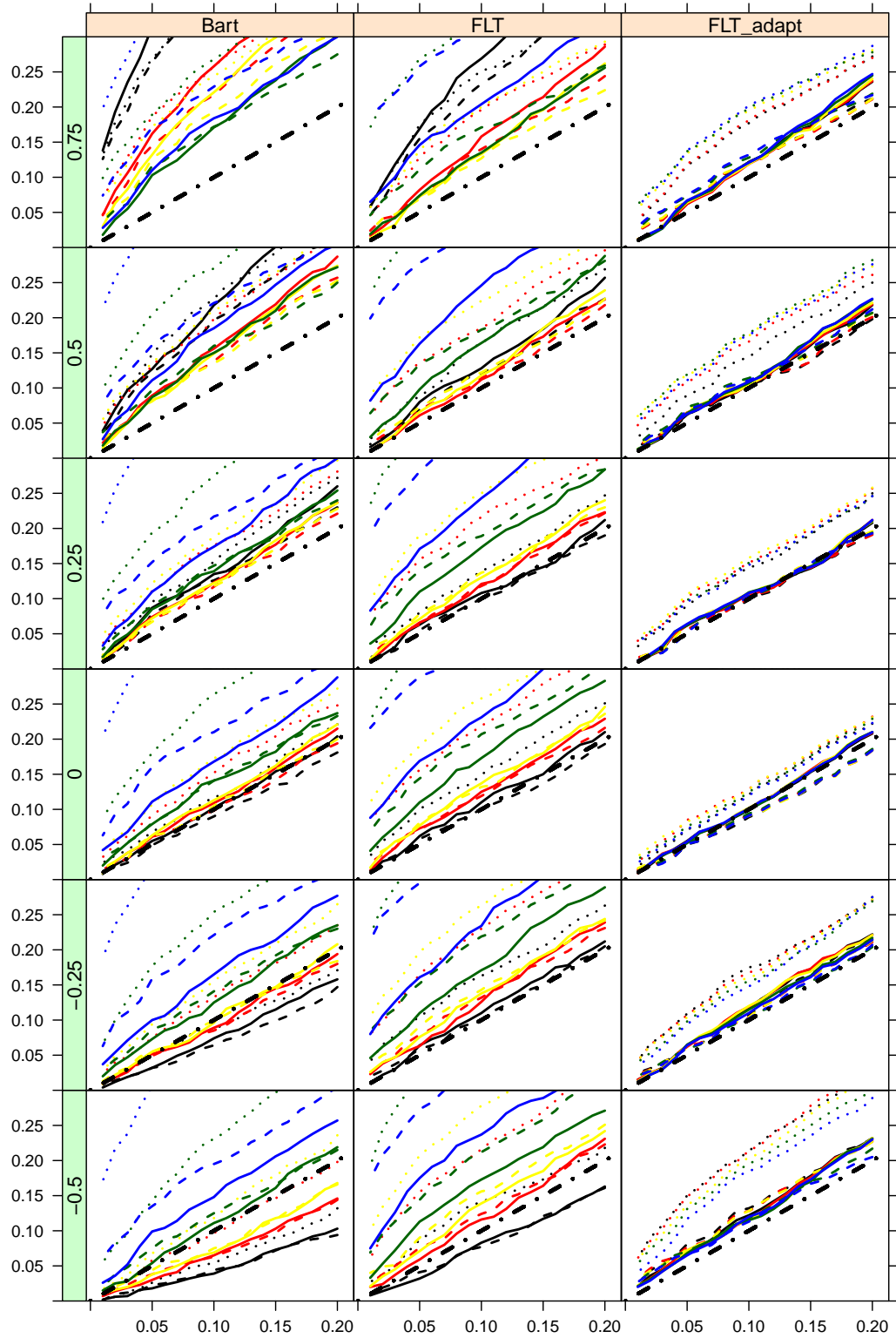


Figure 5: Huber procedure, $\gamma = 0.25$, errors being AR(1) of Laplace innovations with ρ indicated at LHS of each panel.

Huber_Lapl_045

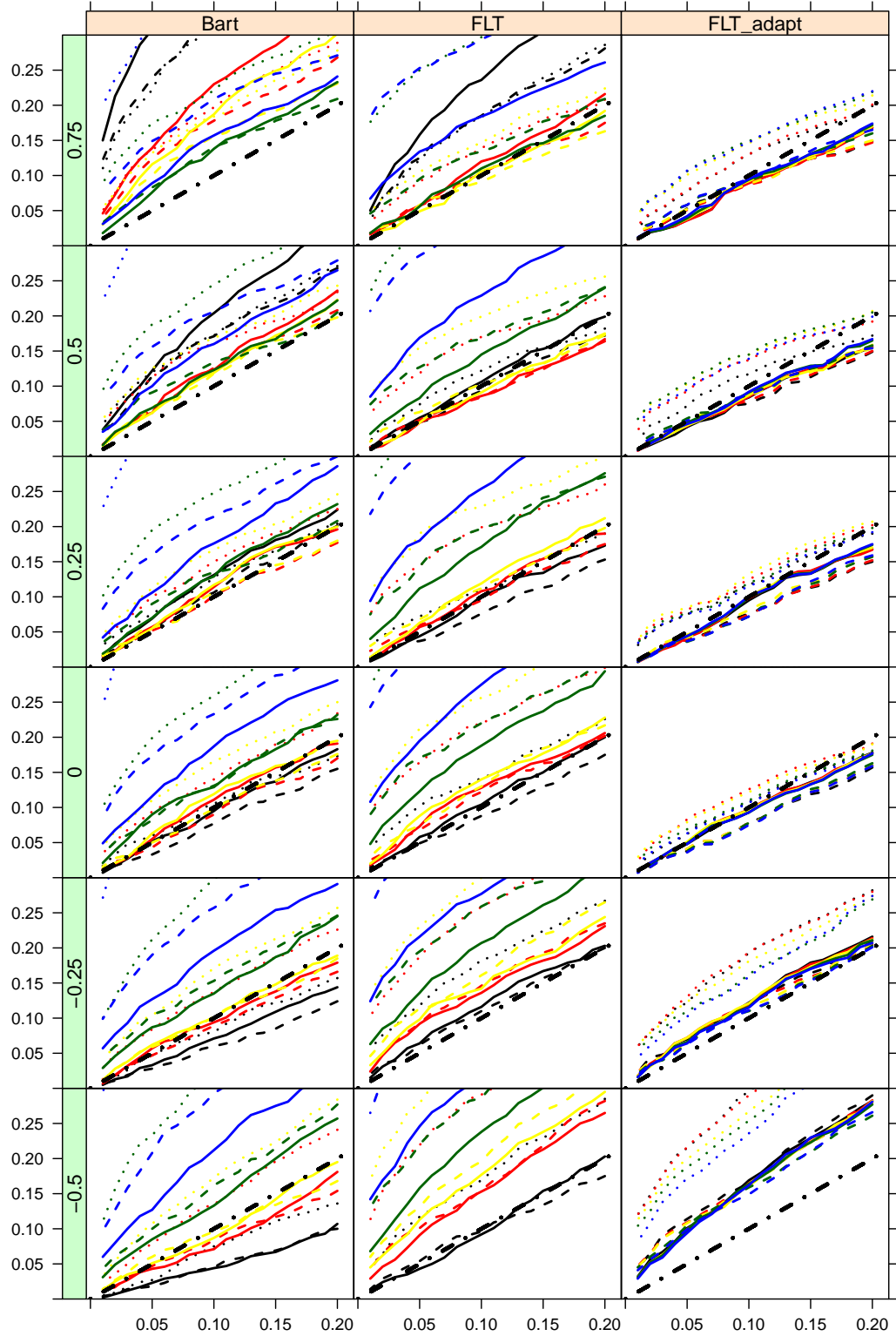


Figure 6: Huber procedure, $\gamma = 0.45$, errors being AR(1) of Laplace innovations with ρ indicated at LHS of each panel.

Huber_t3_0

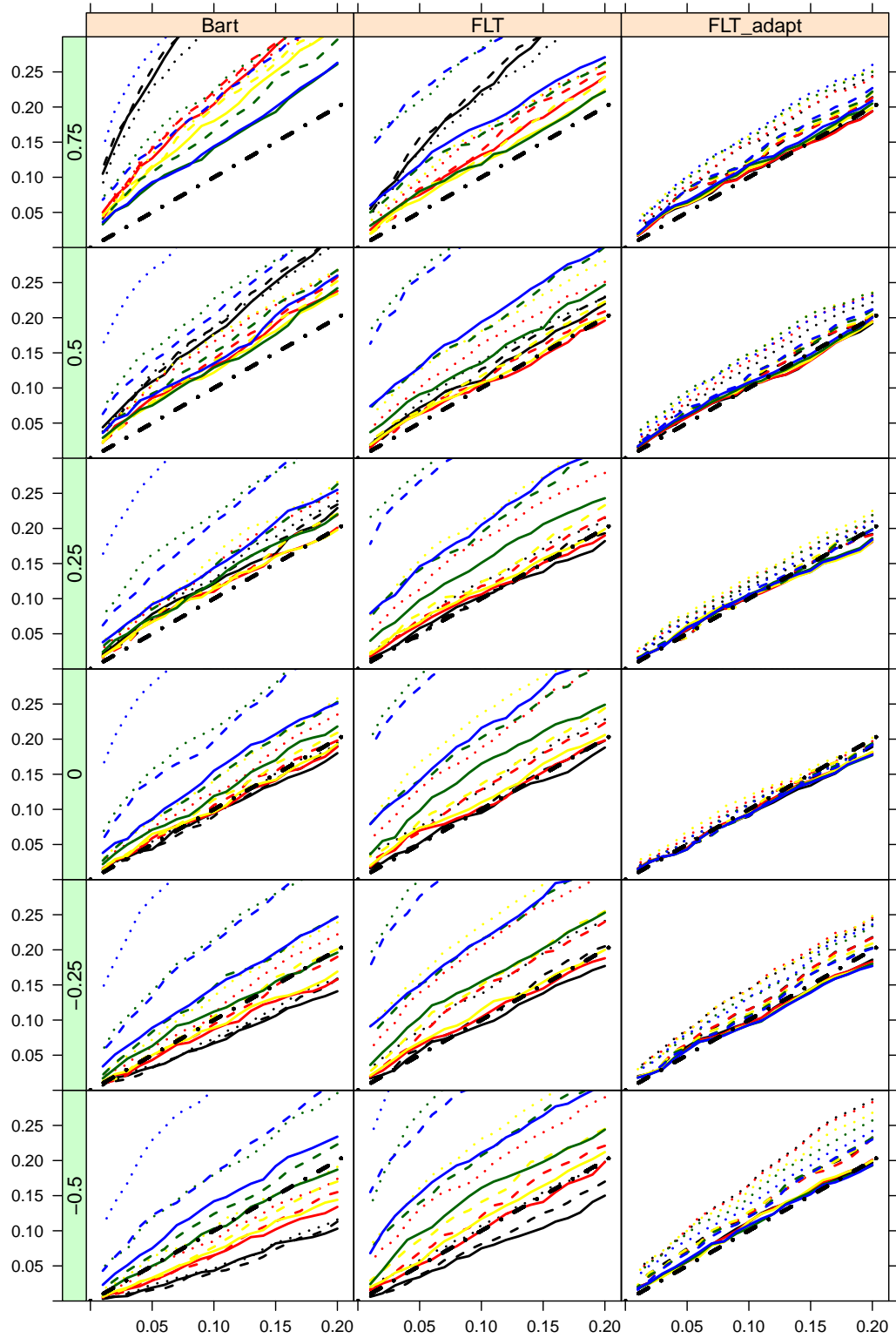


Figure 7: Huber procedure, $\gamma = 0$, errors being AR(1) of t_3 innovations with ρ indicated at LHS of each panel.

Huber_t3_025

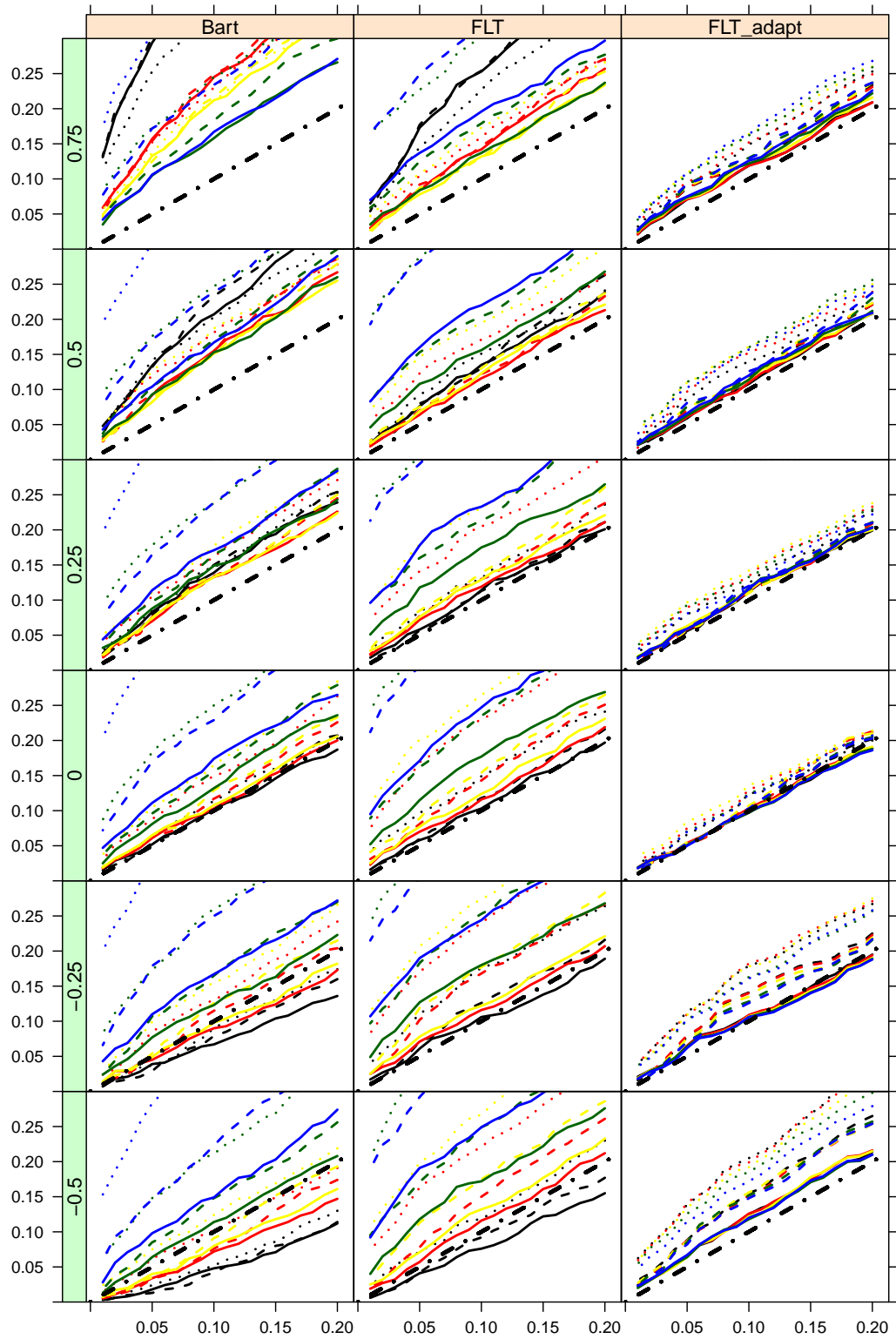


Figure 8: Huber procedure, $\gamma = 0.25$, errors being AR(1) of t_3 innovations with ρ indicated at LHS of each panel.

Huber_t3_045

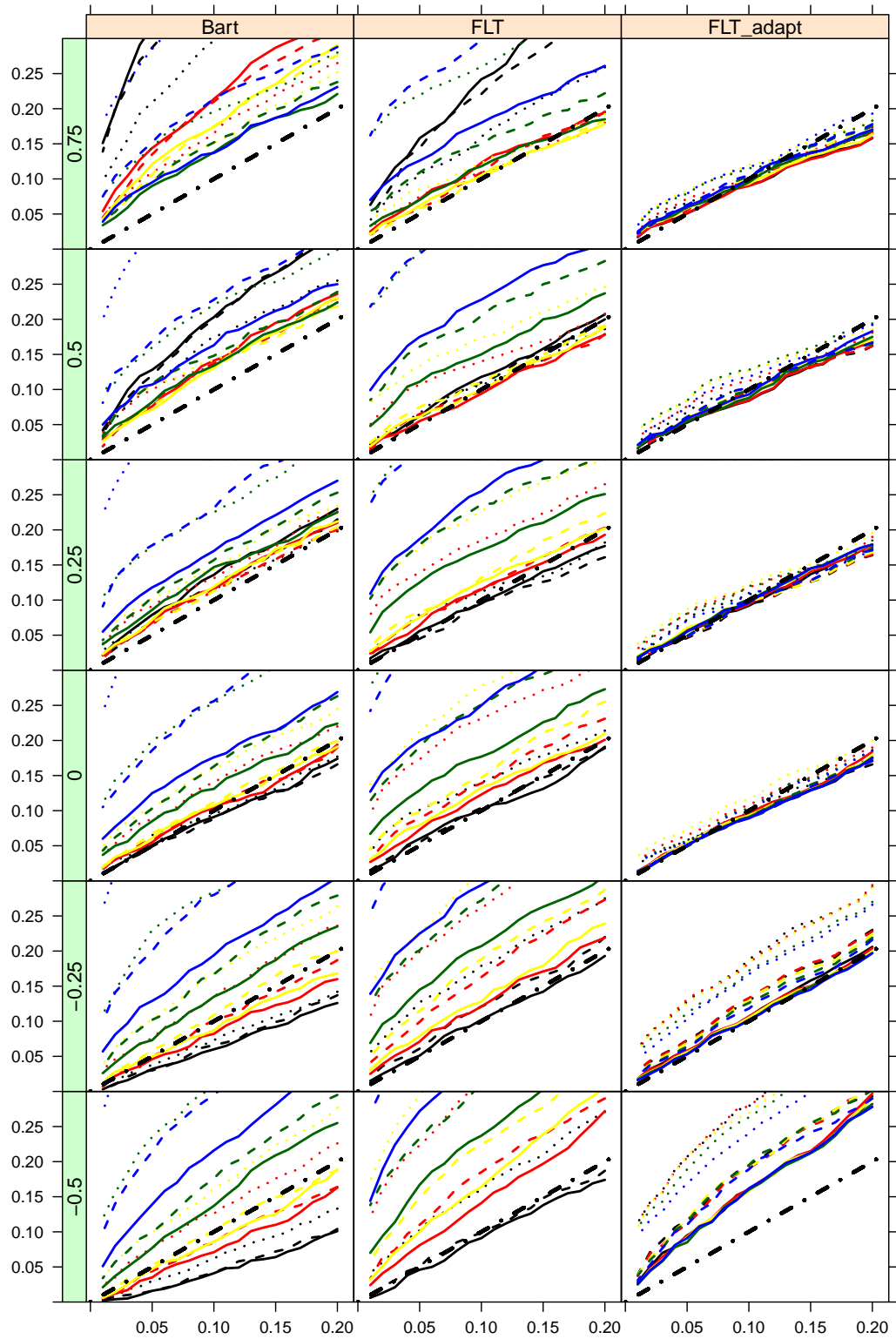


Figure 9: Huber procedure, $\gamma = 0.45$, errors being AR(1) of t_3 innovations with ρ indicated at LHS of each panel.

Huber_MA_0

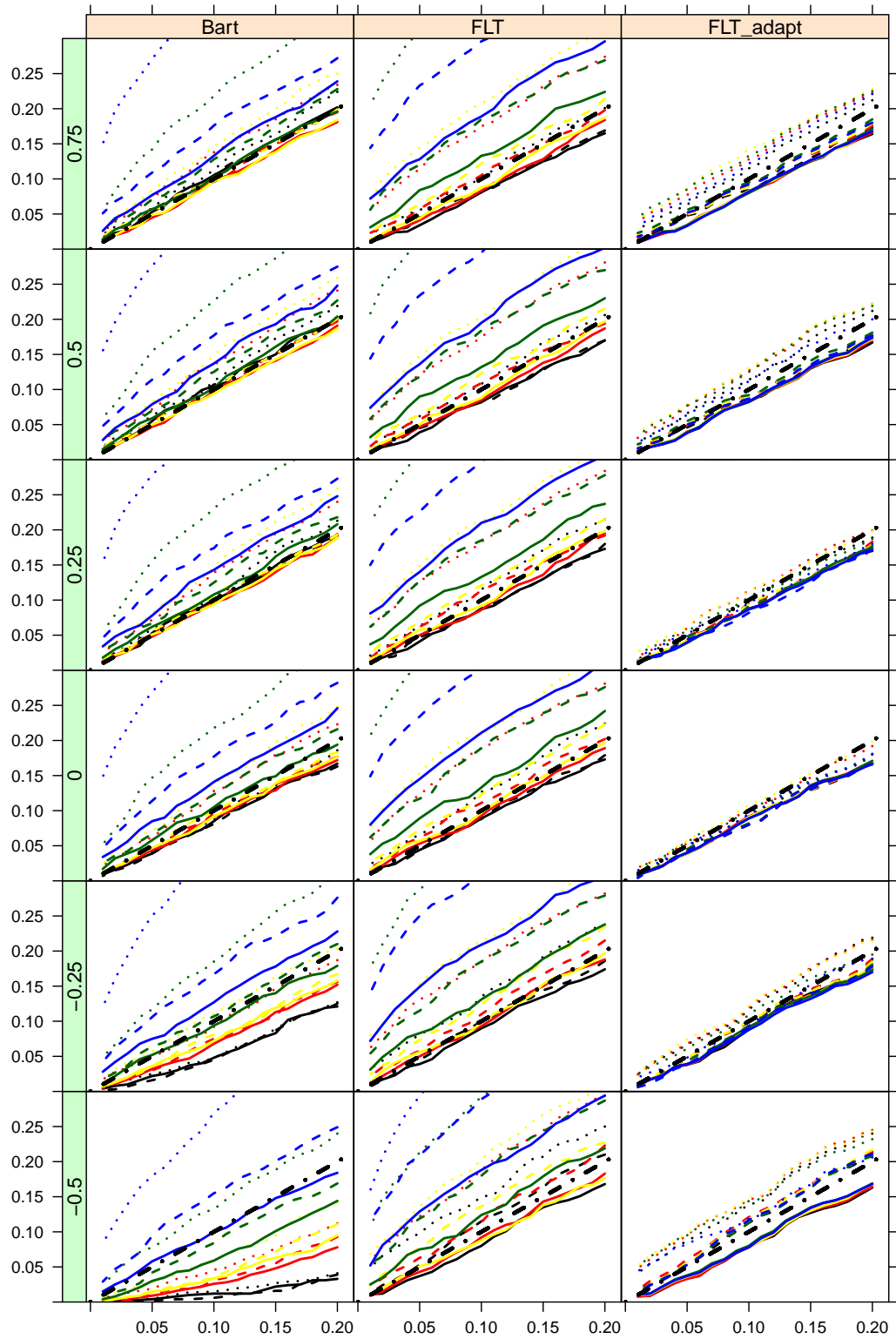


Figure 10: Huber procedure, $\gamma = 0$, errors being MA(1) of $N(0, 1)$ innovations with ρ indicated at LHS of each panel.

Huber_MA_025

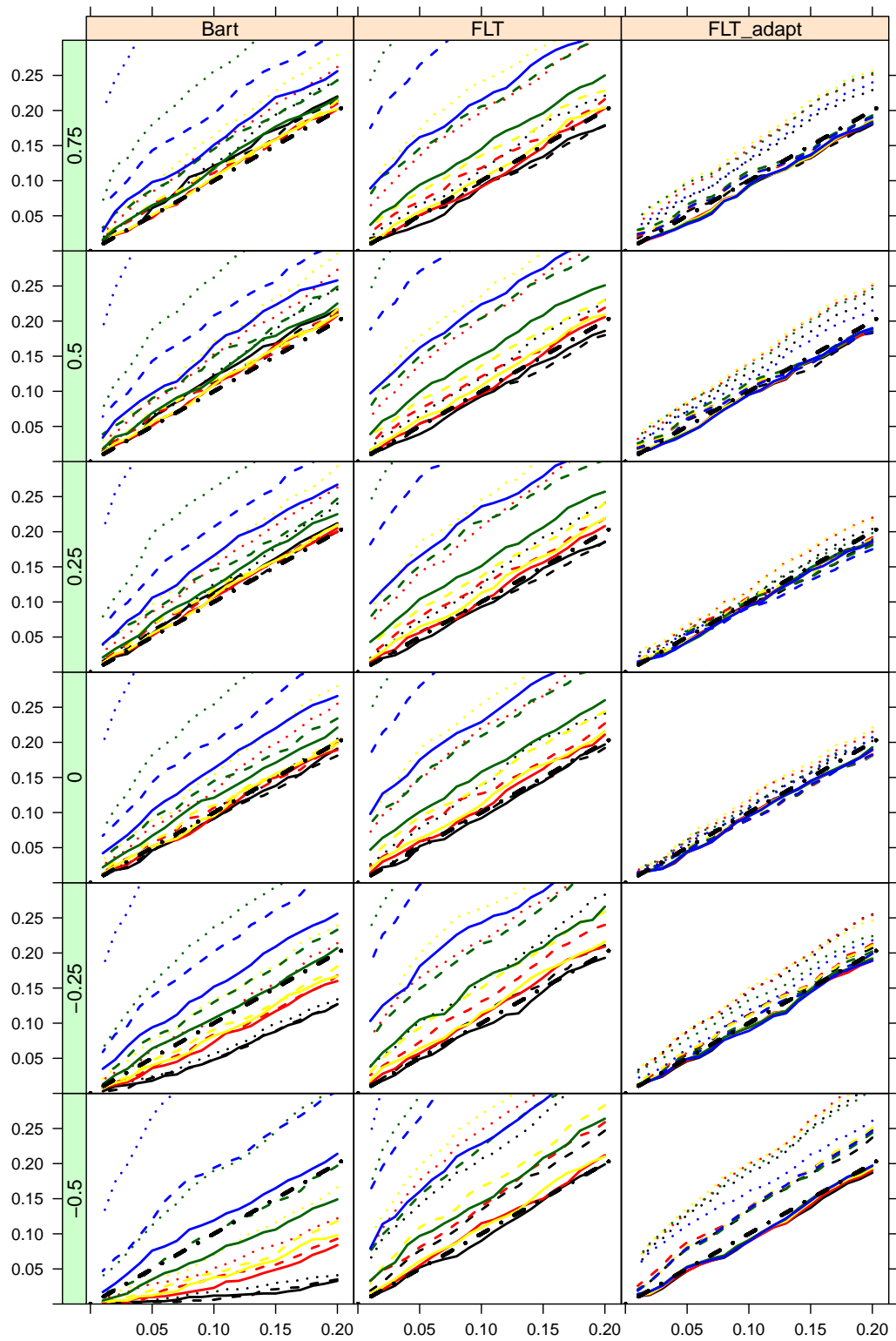


Figure 11: Huber procedure, $\gamma = 0.25$, errors being MA(1) of $N(0, 1)$ innovations with ρ indicated at LHS of each panel.

Huber_MA_045

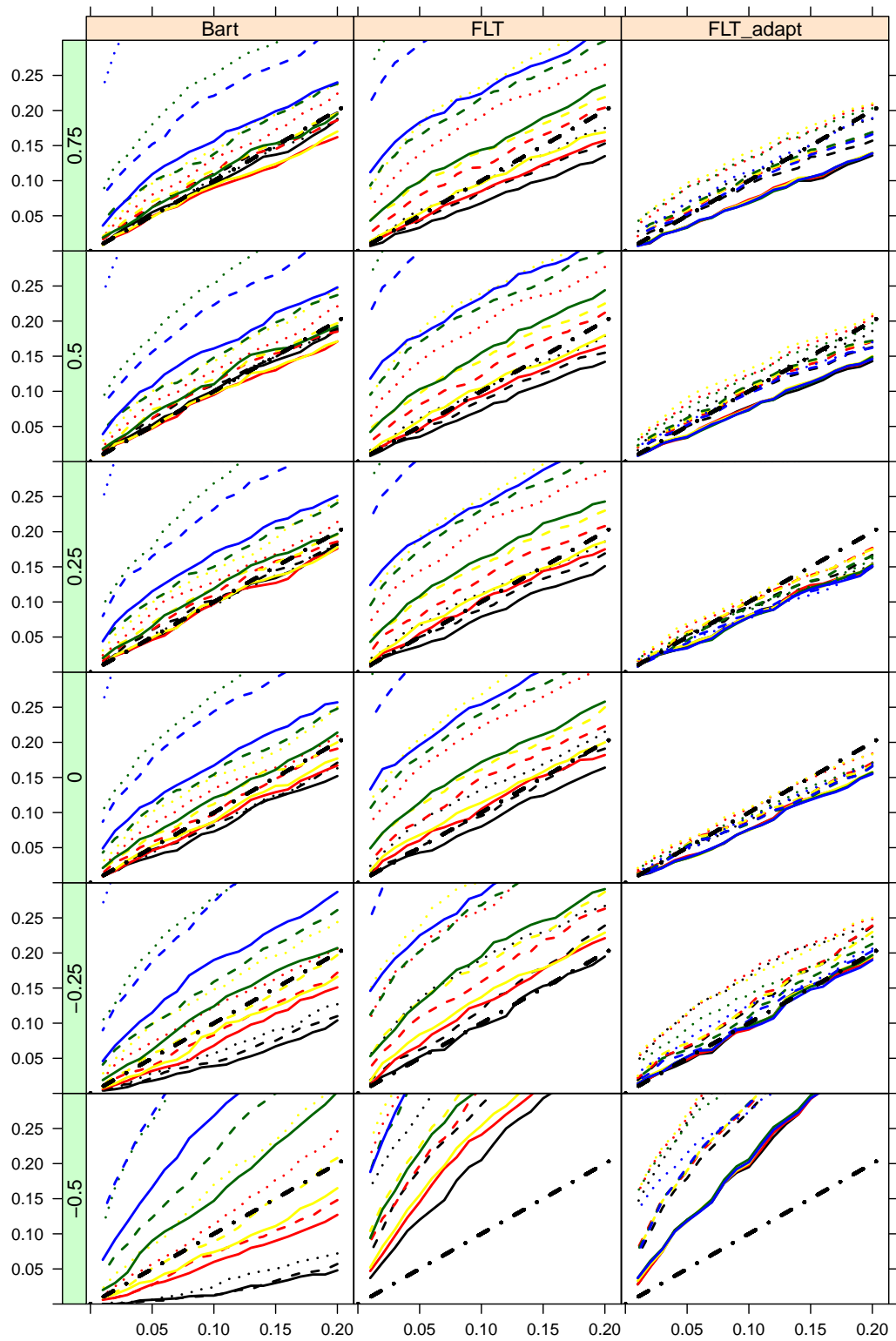


Figure 12: Huber procedure, $\gamma = 0.45$, errors being MA(1) of $N(0, 1)$ innovations with ρ indicated at LHS of each panel.

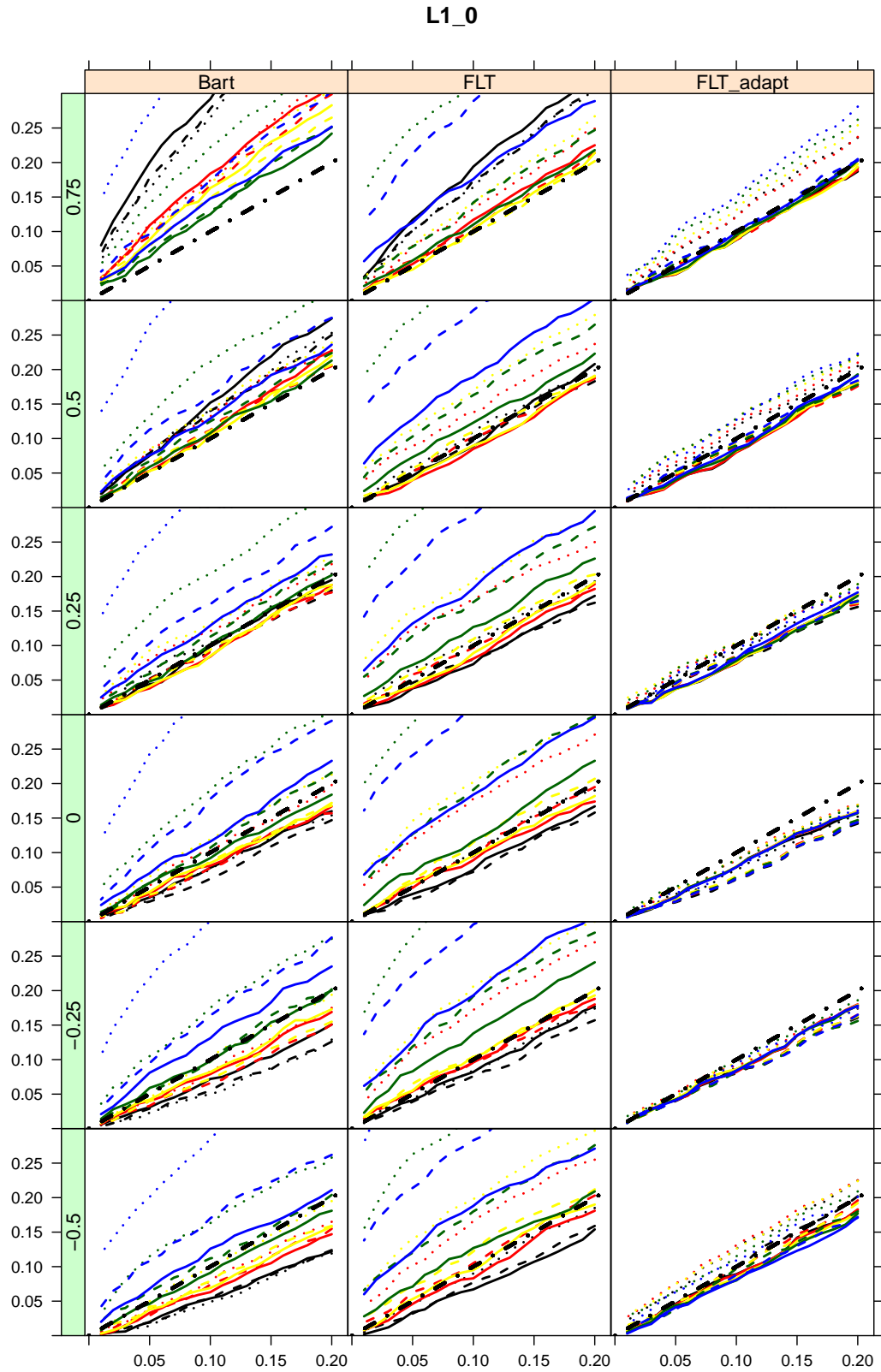


Figure 13: L_1 procedure, $\gamma = 0$, errors being AR(1) of $N(0, 1)$ innovations with ρ indicated at LHS of each panel.

L1_025

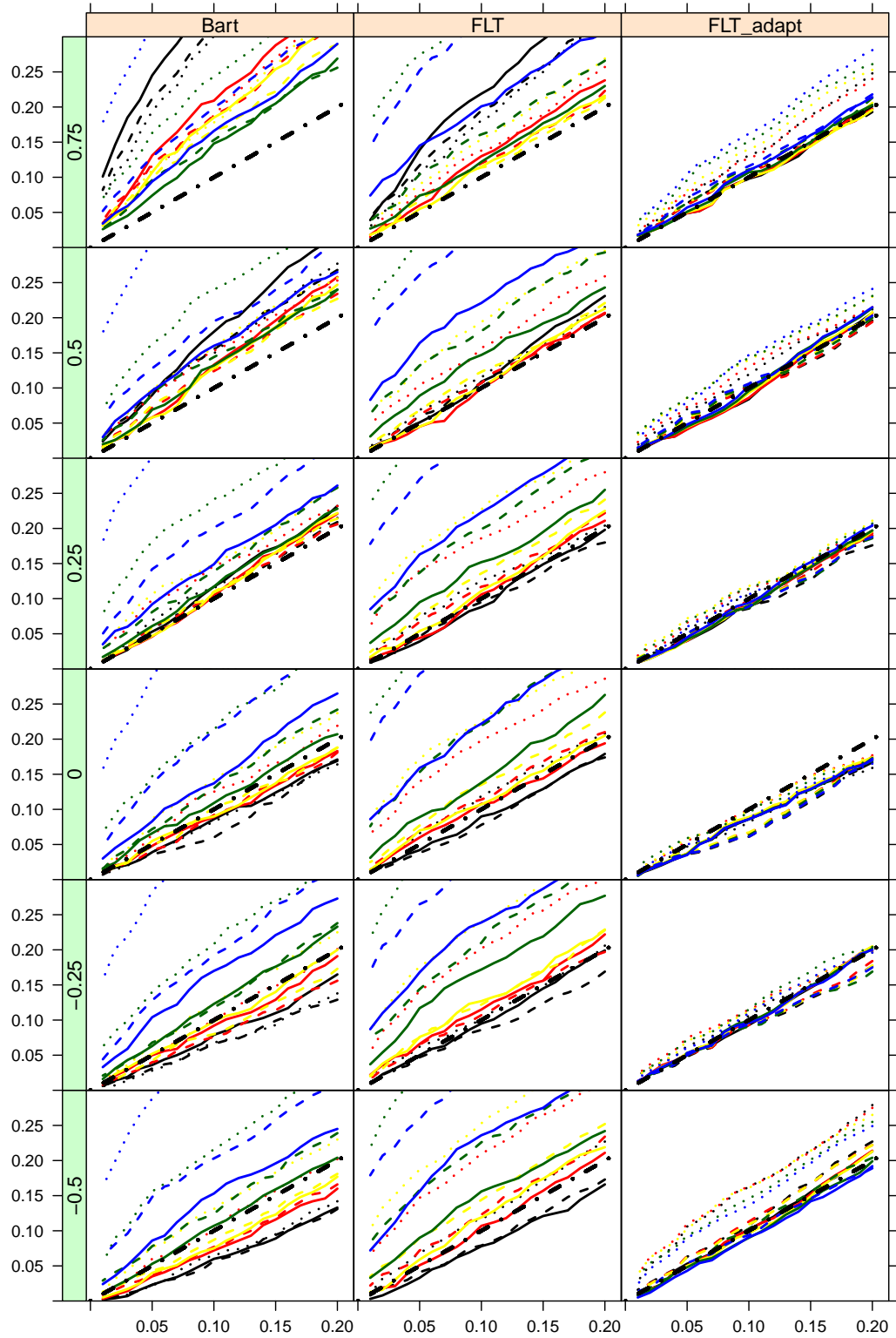


Figure 14: L_1 procedure, $\gamma = 0.25$, errors being AR(1) of $N(0, 1)$ innovations with ρ indicated at LHS of each panel.

L1_045

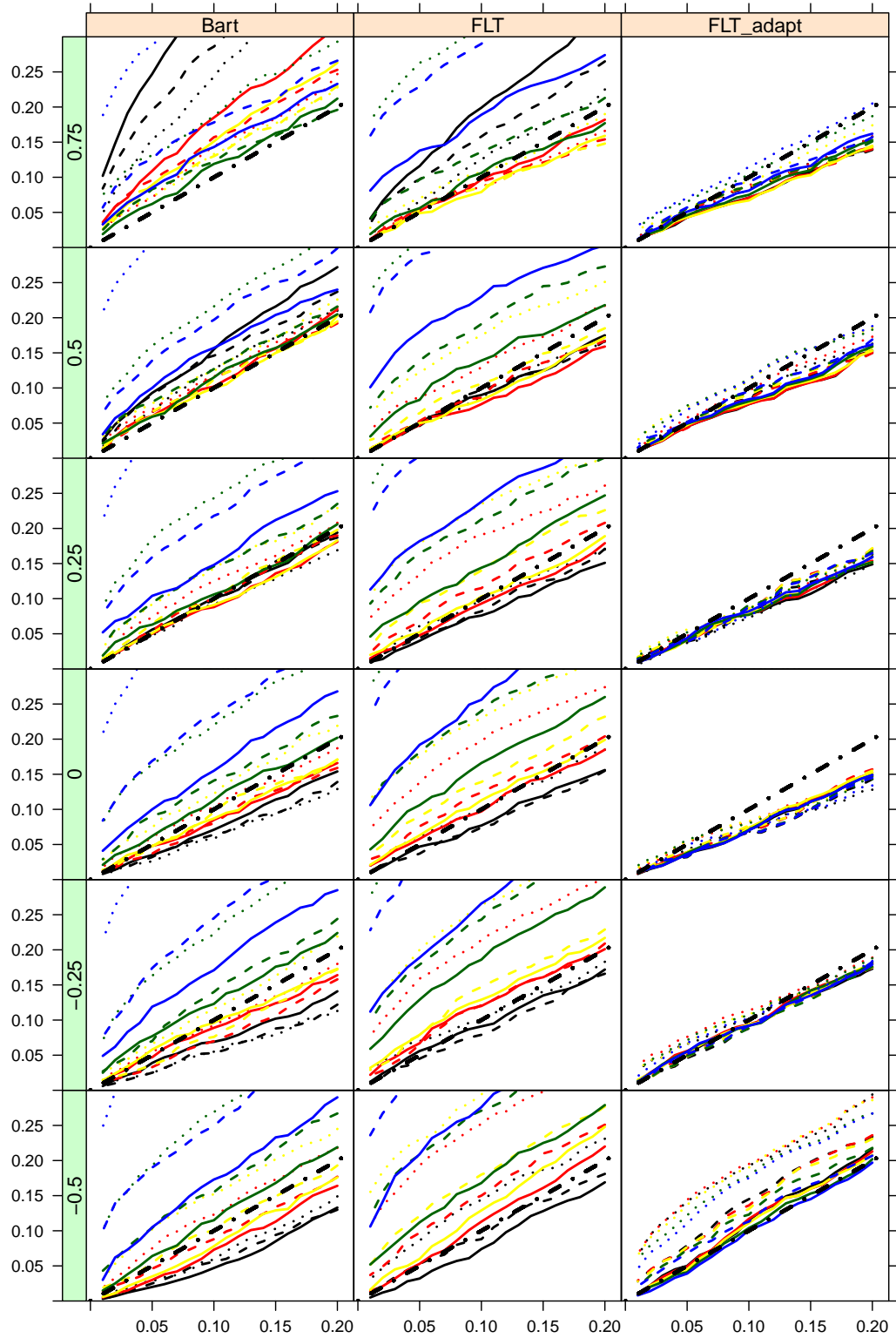


Figure 15: L_1 procedure, $\gamma = 0.45$, errors being AR(1) of $N(0, 1)$ innovations with ρ indicated at LHS of each panel.

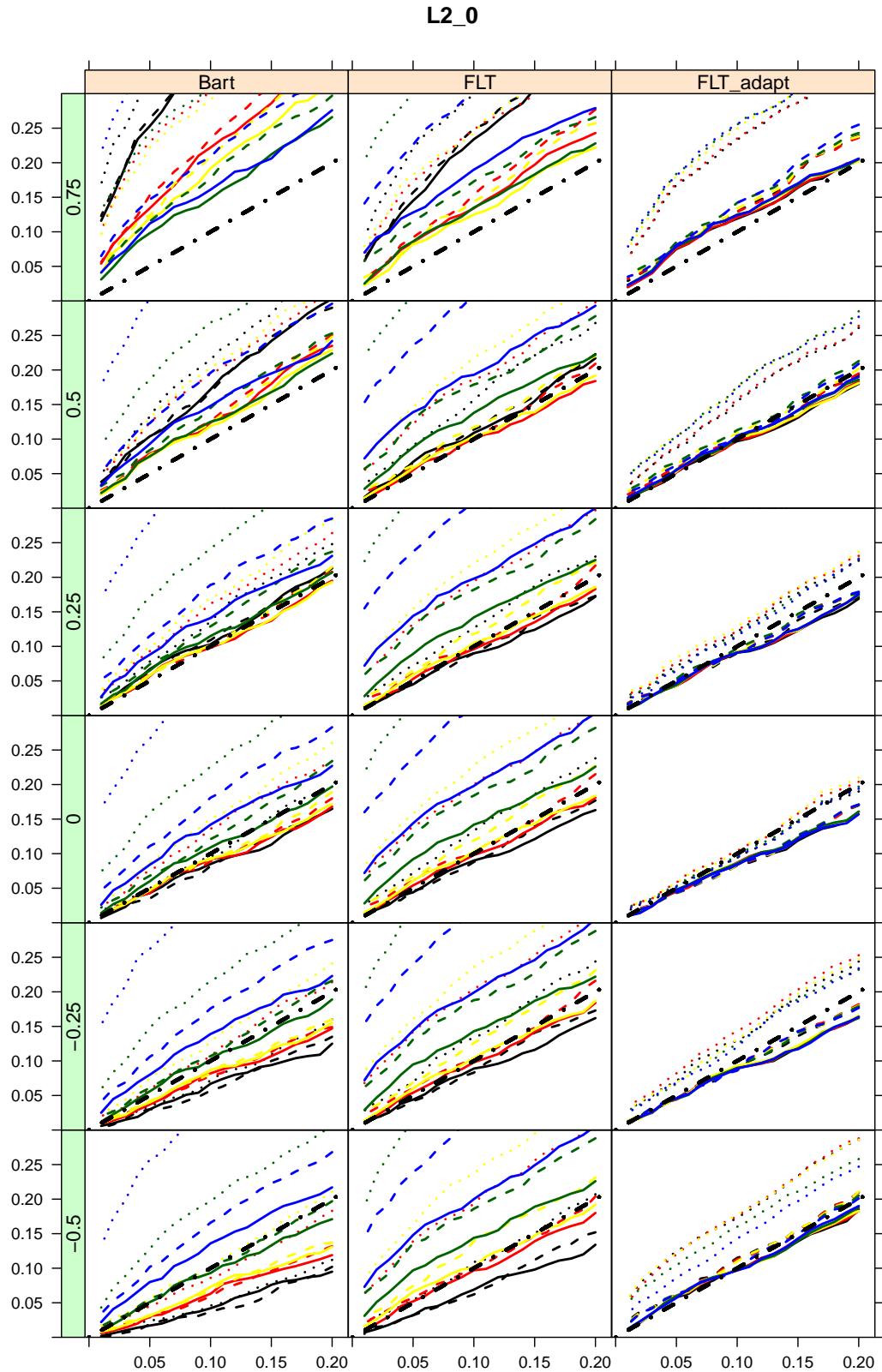


Figure 16: L_2 procedure, $\gamma = 0$, errors being AR(1) of $N(0, 1)$ innovations with ρ indicated at LHS of each panel.

L2_025

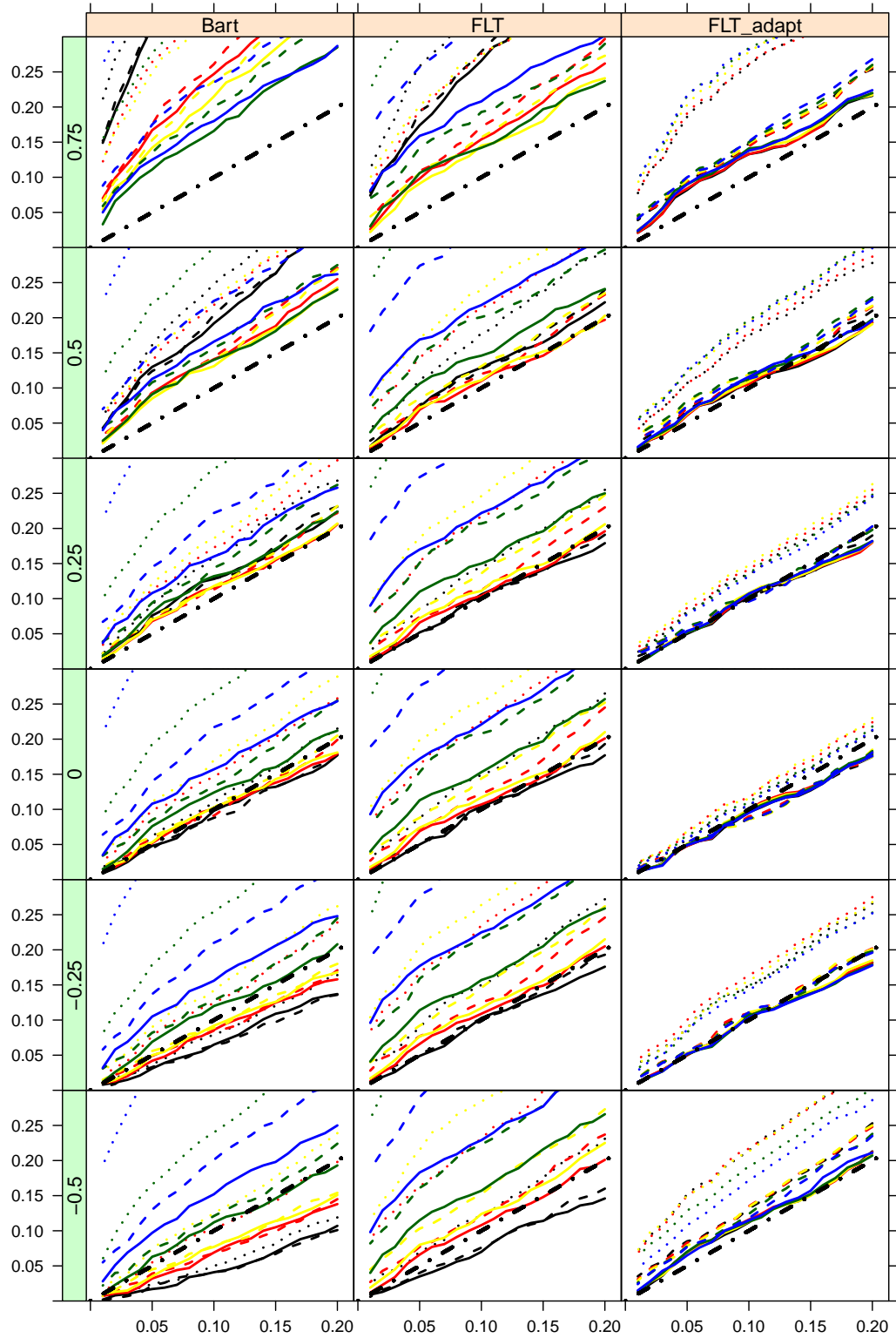


Figure 17: L_2 procedure, $\gamma = 0.25$, errors being $AR(1)$ of $N(0, 1)$ innovations with ρ indicated at LHS of each panel.

L2_045

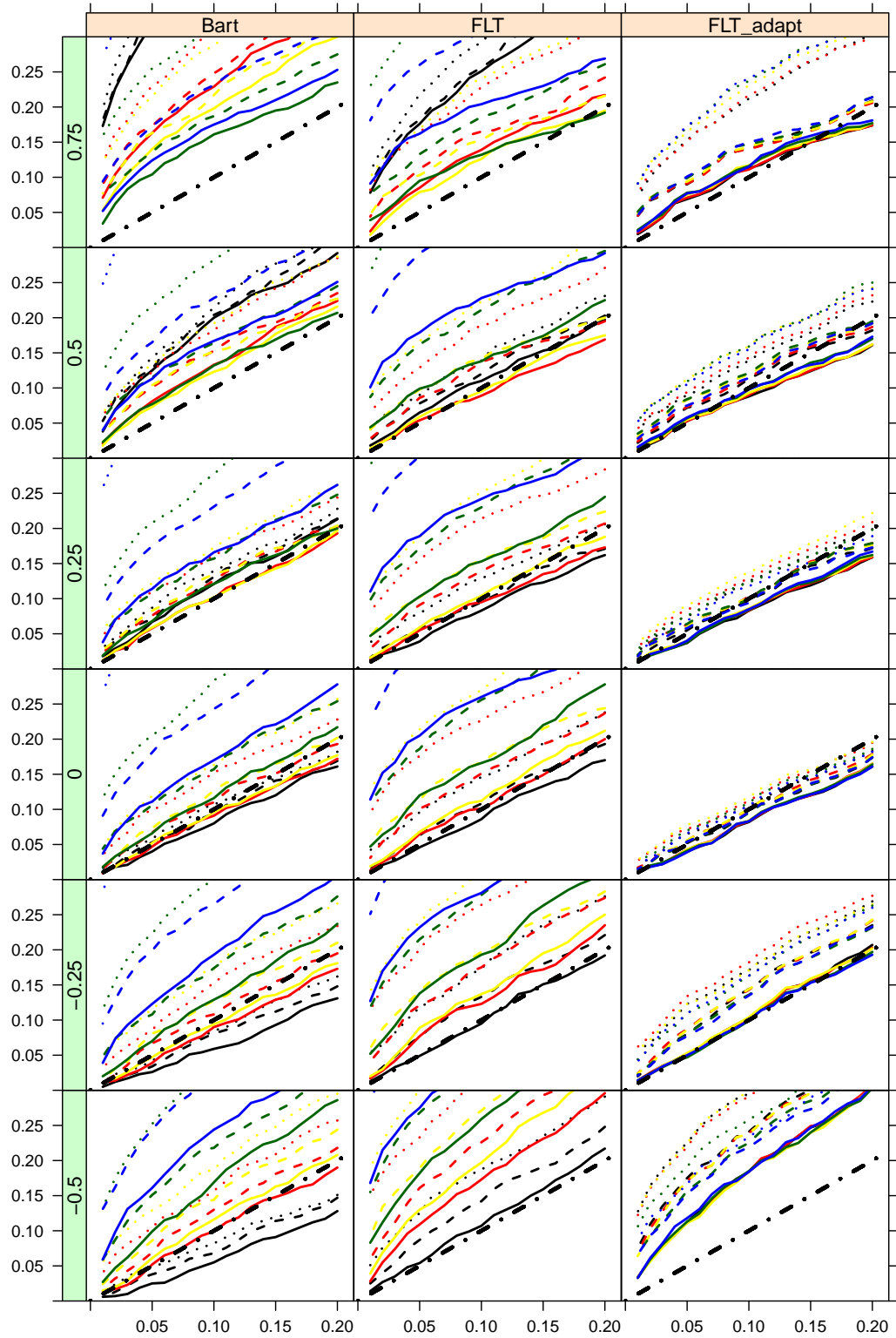


Figure 18: L_2 procedure, $\gamma = 0.45$, errors being AR(1) of $N(0, 1)$ innovations with ρ indicated at LHS of each panel.

1.2 Figure 6.2

Here we show analogues of Figure 6.2 presenting kernel density estimates of the LRV for different estimators for all procedures considered. We start with the Huber procedure, which is included in the thesis and continue with the L_1 and L_2 procedures.

Errors form AR(1) of $N(0, 1)$ innovations with ρ indicated at LHS of each panel. Vertical black line represent true LRV. Please note different scale of each panel.

Λ_m : 4 - black, 8 - red, 10- yellow, 20 - green, 40 - blue and accordingly for FLT adapt;
 m : 80 - dotted, 200 - dashed, 400 - solid.

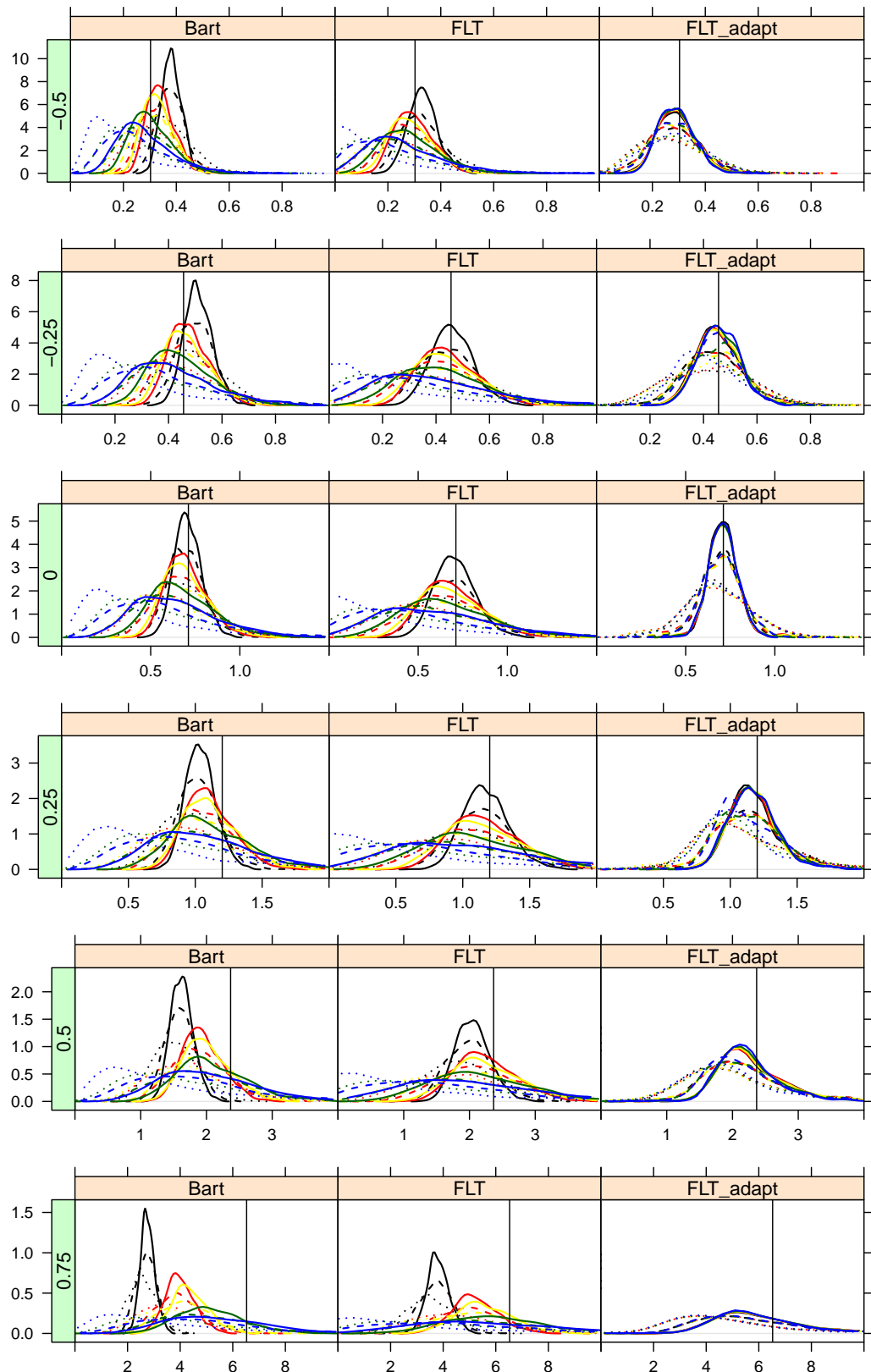


Figure 19: Kernel density estimates of the LRV for different estimators, Huber procedure.

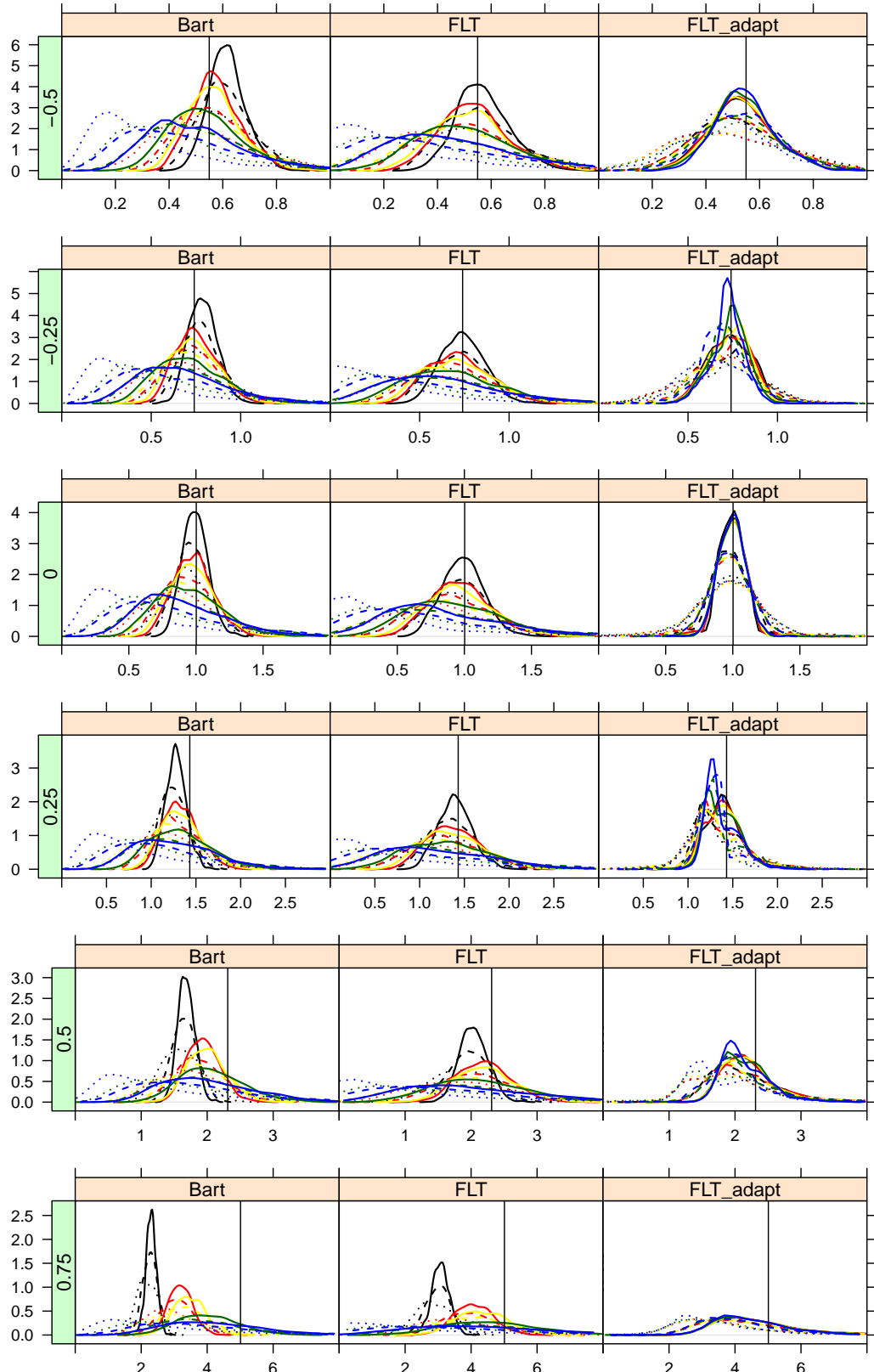


Figure 20: Kernel density estimates of the LRV for different estimators, L_1 procedure.

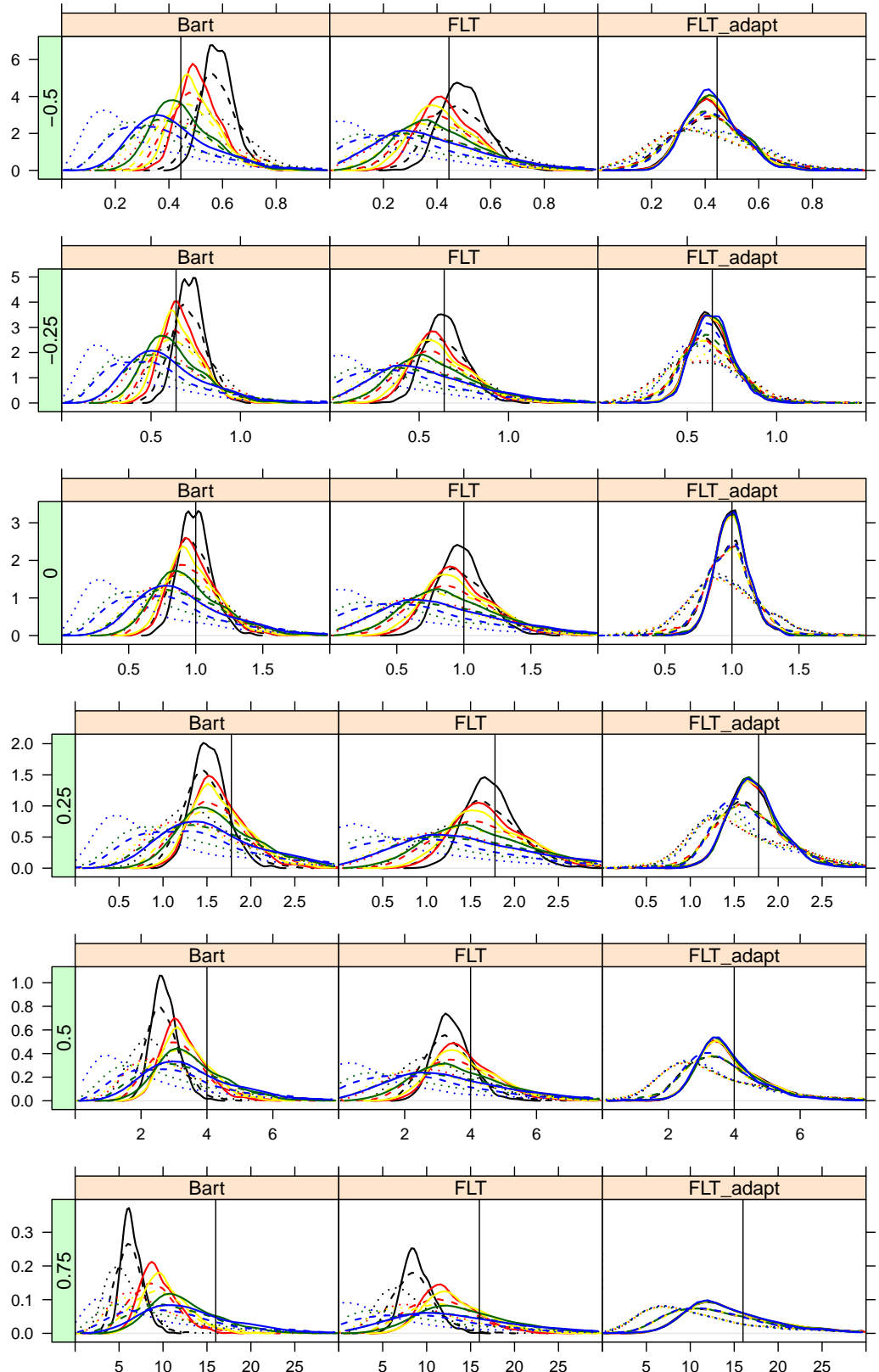


Figure 21: Kernel density estimates of the LRV for different estimators, L_2 procedure.

1.3 Figure 6.3

Here we present histograms of number of lags Λ_m selected by the adaptive FLT estimator for different procedures and constants K and c . Errors form AR(1) of $N(0, 1)$ innovations with ρ indicated at LHS of each panel, the length of the training period m is in columns.

The figure from thesis is presented first, i.e. the Huber procedure, for $K = 3$, $c = 1.4$. Then we use $K = 1$, $c = 1$ and $K = 5$, $c = 2$ for this procedure. Finally we show figures for L_1 and L_2 procedures with $K = 3$, $c = 1.4$.

K=3, c=1.4

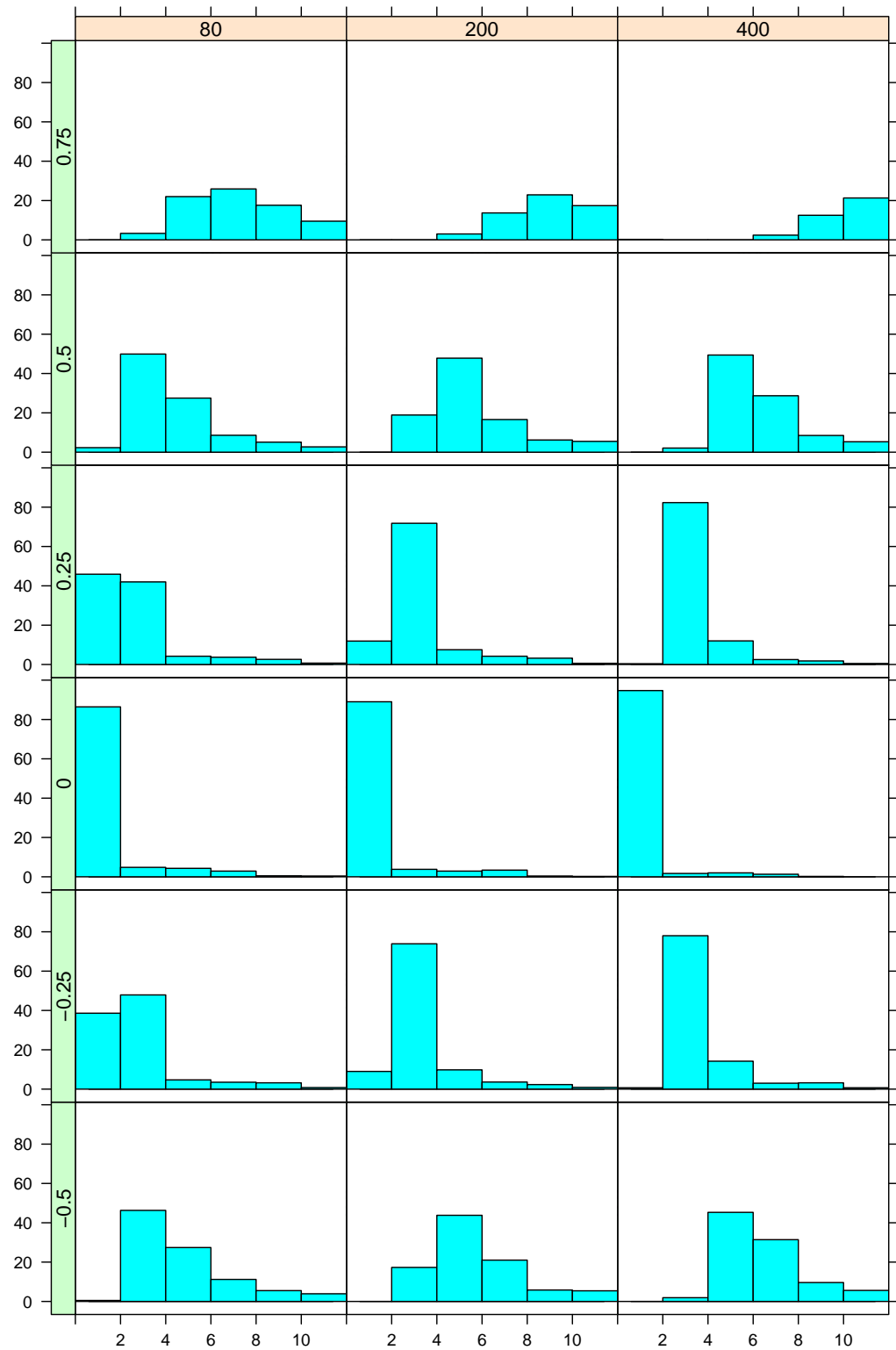


Figure 22: Huber procedure, for $K = 3$, $c = 1.4$.

K=1, c=1

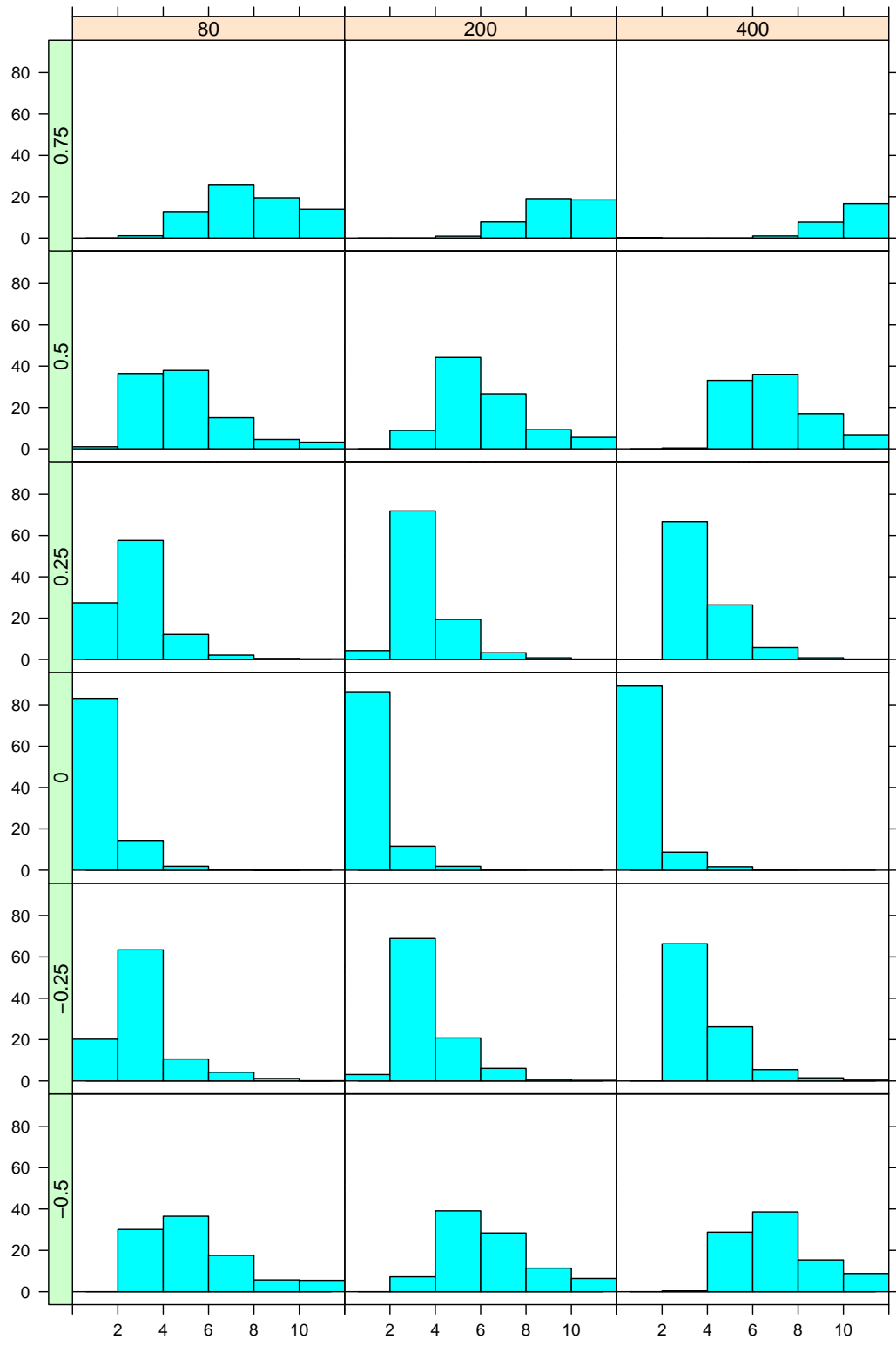


Figure 23: Huber procedure, for $K = 1, c = 1$.

K=5, c=2

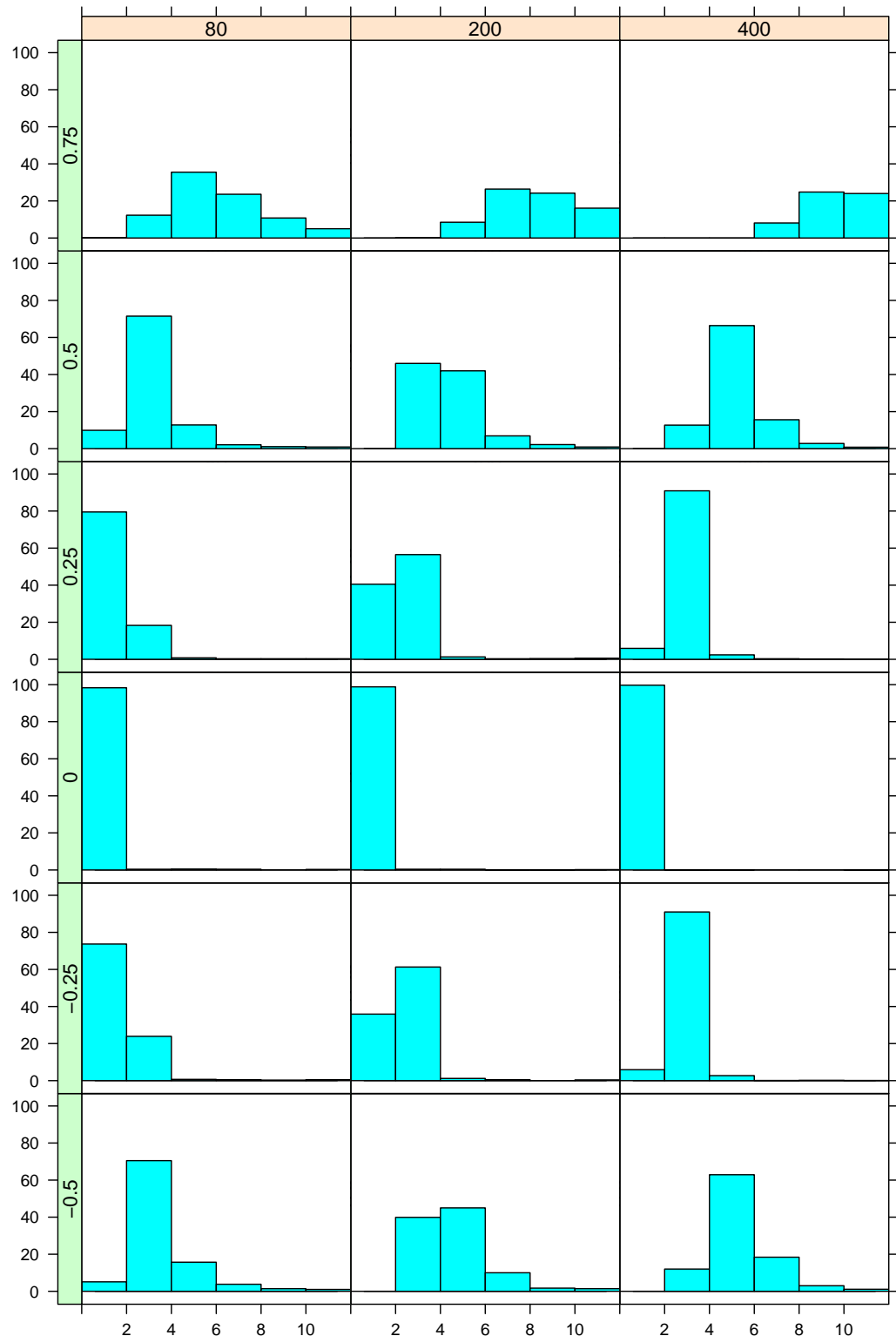


Figure 24: Huber procedure, for $K = 5$, $c = 2$.

K=3, c=1.4

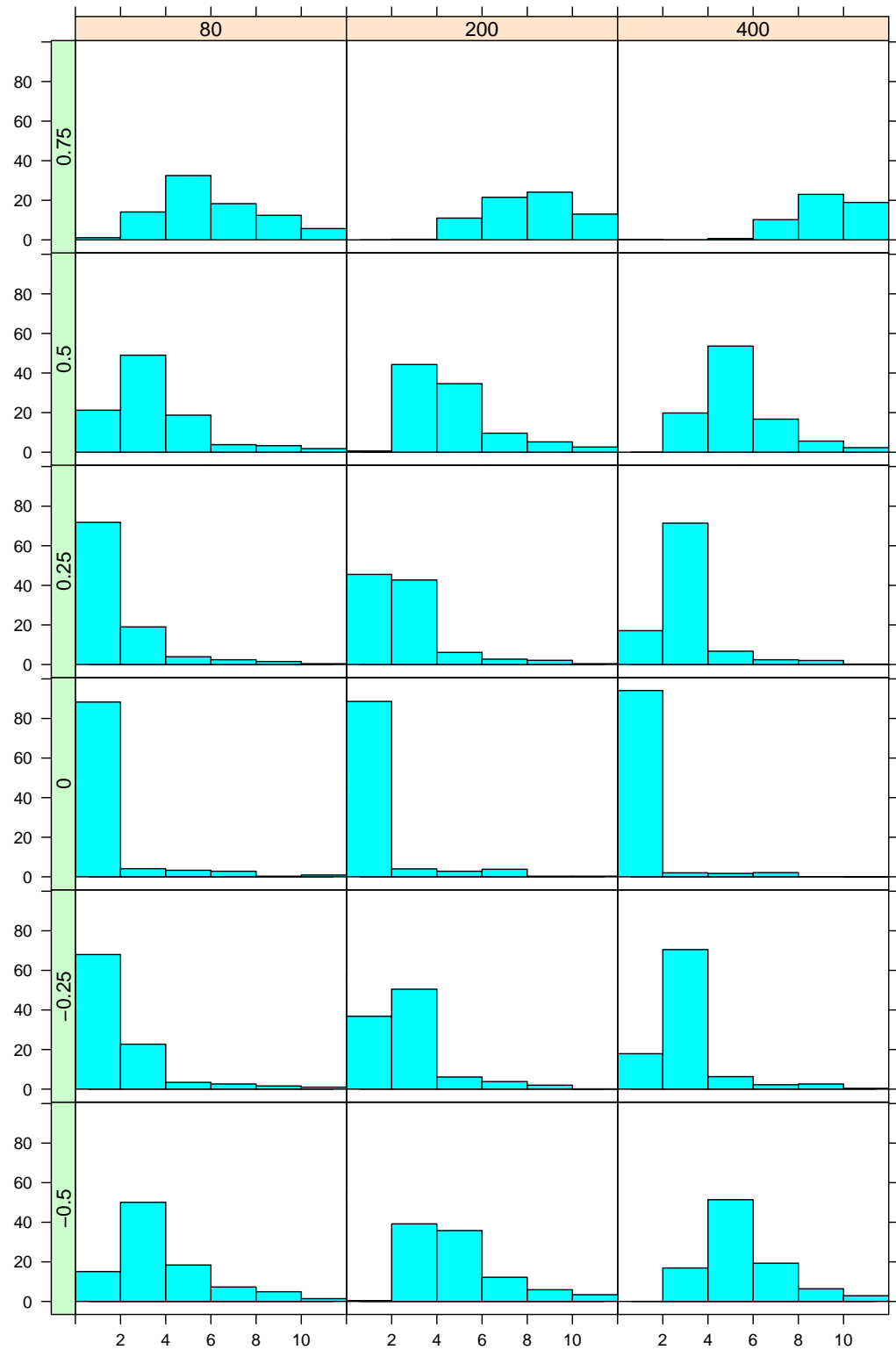


Figure 25: L_1 procedure, for $K = 3$, $c = 1.4$.

K=3, c=1.4

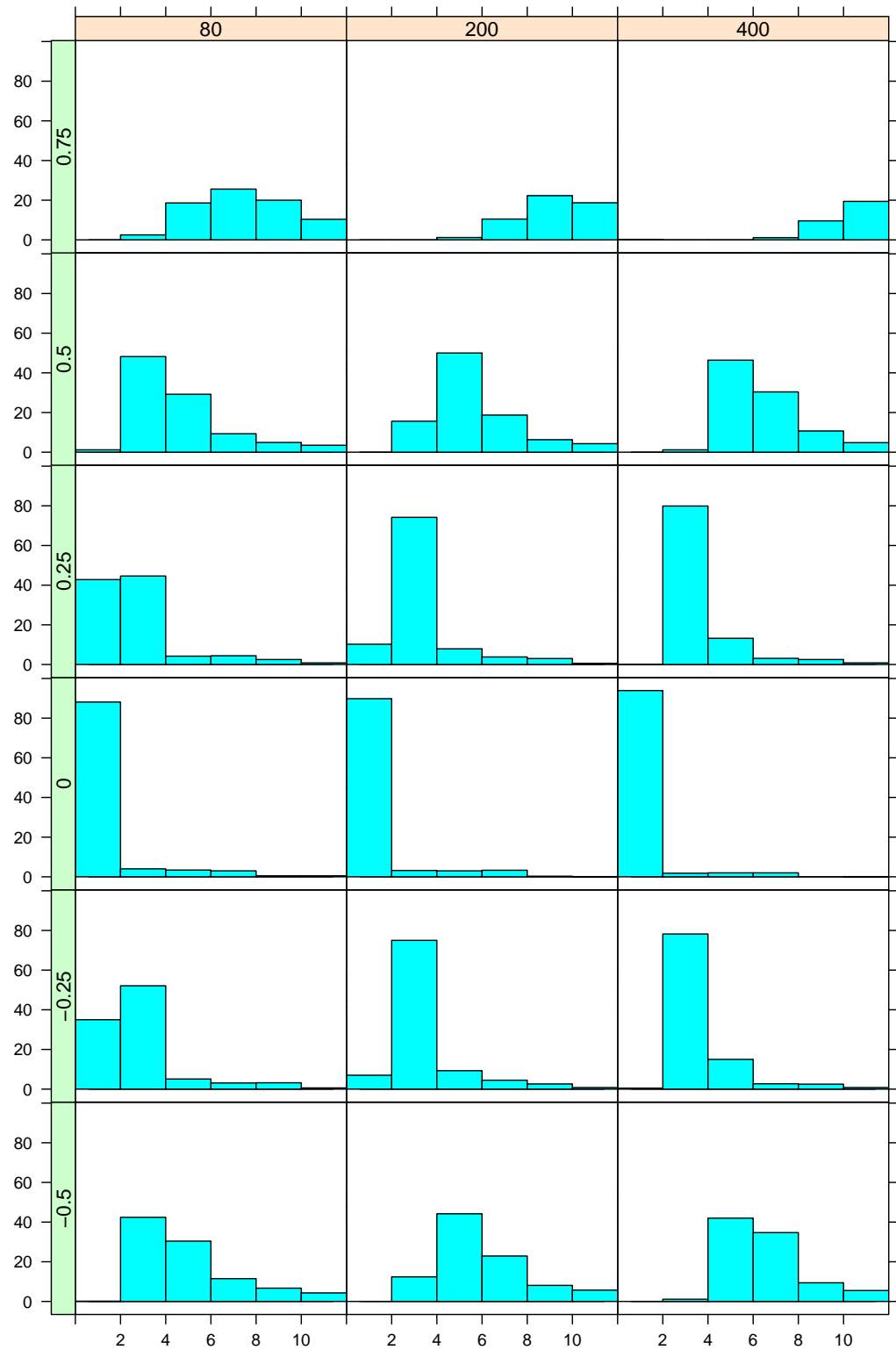


Figure 26: L_2 procedure, for $K = 3$, $c = 1.4$.

1.4 Figure 6.7

In this subsection we present the robustness aspects of the procedures and the influence of tuning constant γ . Following figures show SPC for different procedures with adaptive FLT estimator under H_0 . We start with $\gamma = 0.25$, then $\gamma = 0$ and finish with 0.45.

H0_robust_025

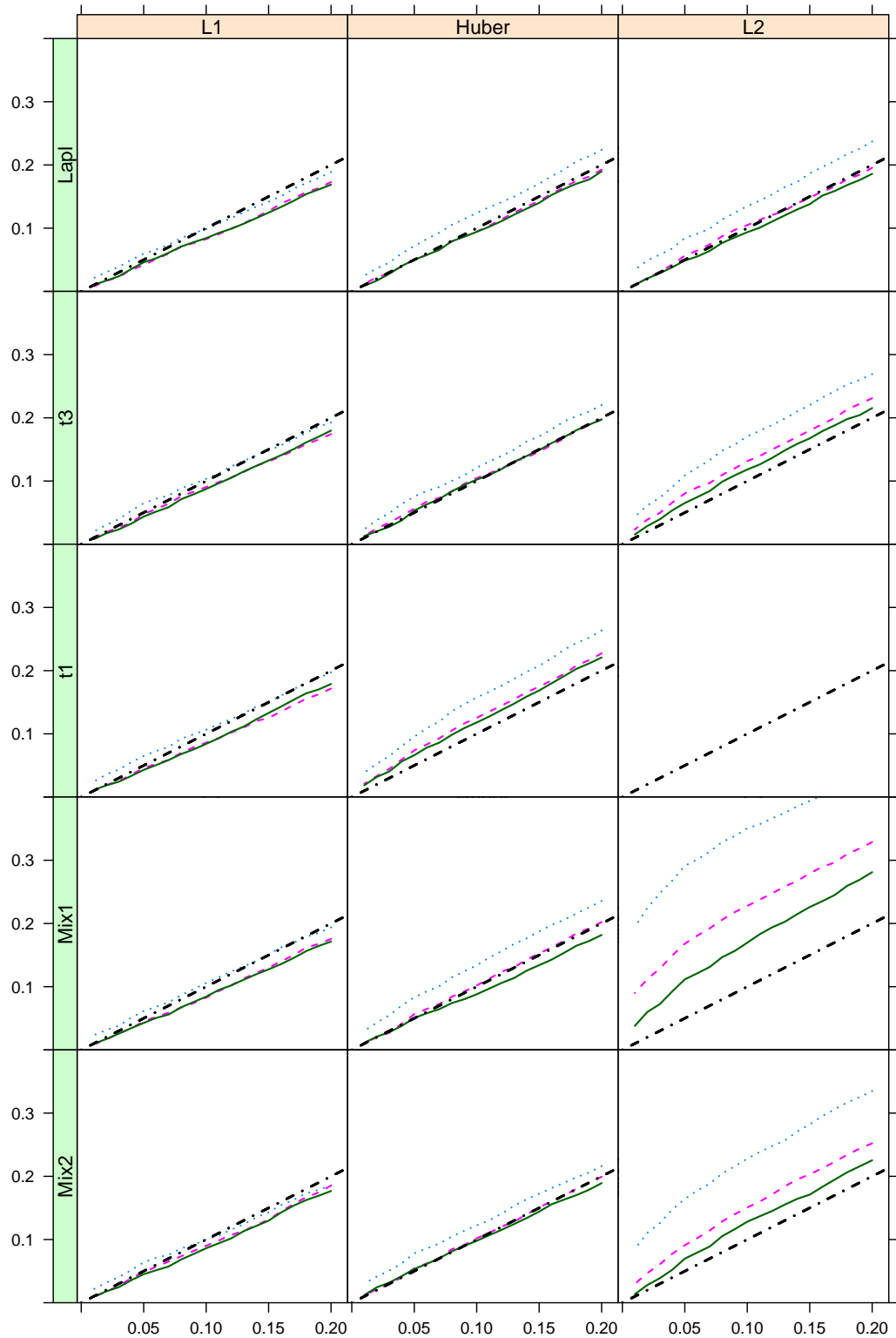


Figure 27: SPC for different procedures with adaptive FLT estimator under H_0 , different distribution of errors in each panel, $\gamma = 0.25$.
 m : 80 - dotted, 200 - dashed, 400 - solid.

H0_robust_0

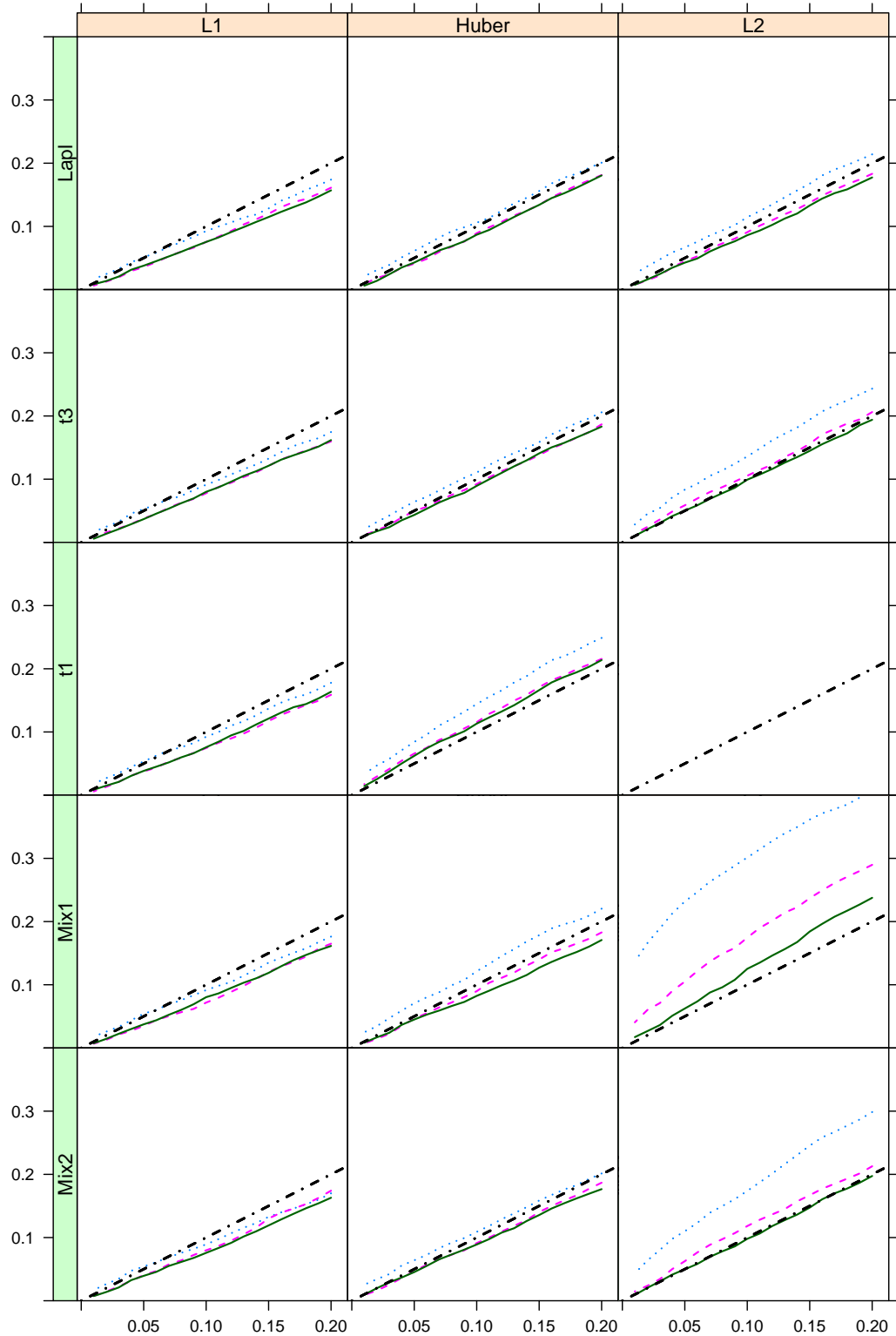


Figure 28: SPC for different procedures with adaptive FLT estimator under H_0 , different distribution of errors in each panel, $\gamma = 0$.
 $m : 80$ - dotted, 200 - dashed, 400 - solid.

H0_robust_045

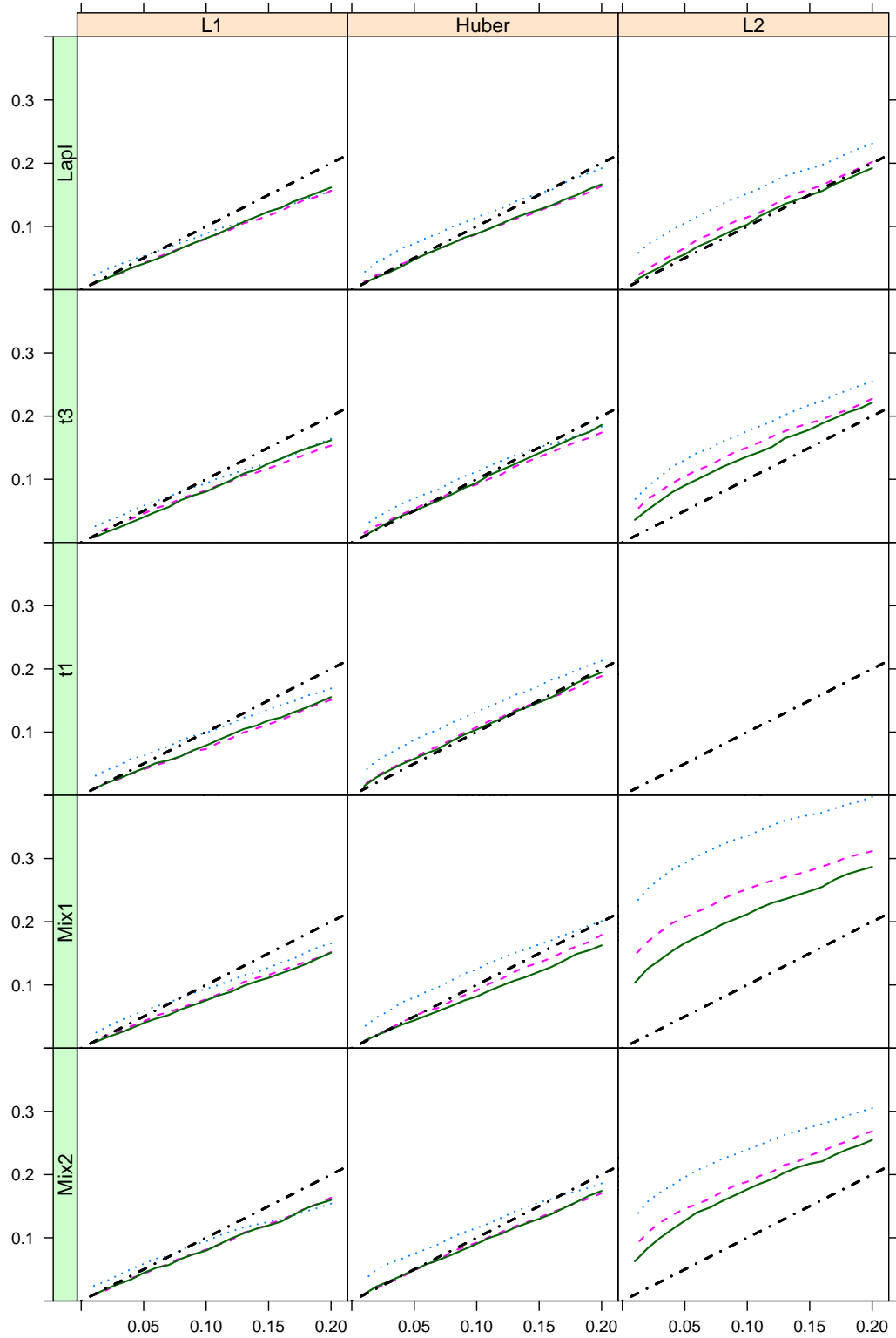


Figure 29: SPC for different procedures with adaptive FLT estimator under H_0 , different distribution of errors in each panel, $\gamma = 0.45$.
 $m : 80$ - dotted, 200 - dashed, 400 - solid.

2 Multivariate Location Model

In this section we compare figures obtained with adaptive Quadratic Spectral kernel LRV estimator with those using FLT kernel with fixed $\Lambda_m = 4$. We start with the null hypothesis (i.e. Figure 6.15 of the thesis), which is followed by alternatives, where also different kinds are presented.

2.1 Figure 6.15

SPC for different procedures under H_0 , with adaptive QS estimator or fixed FLT one, different distributions of errors in each panel, $\gamma = 0.25$.

H0_AdP_12_2000

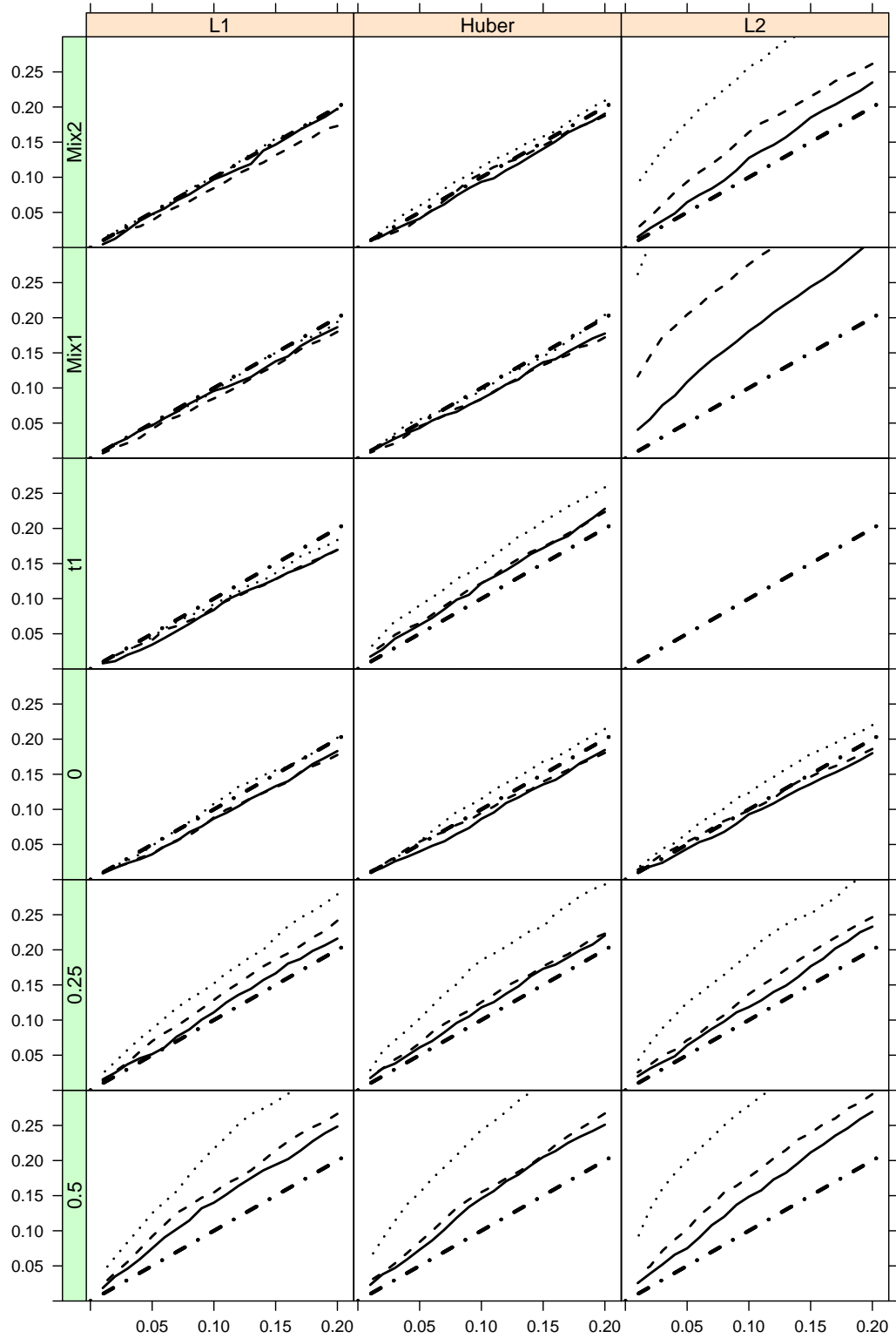


Figure 30: SPC for different procedures with adaptive QS estimator under H_0 , different distributions of errors in each panel, $\gamma = 0.25$.
 $m : 80$ - dotted, 200 - dashed, 400 - solid.

H0_FLT_12_2000

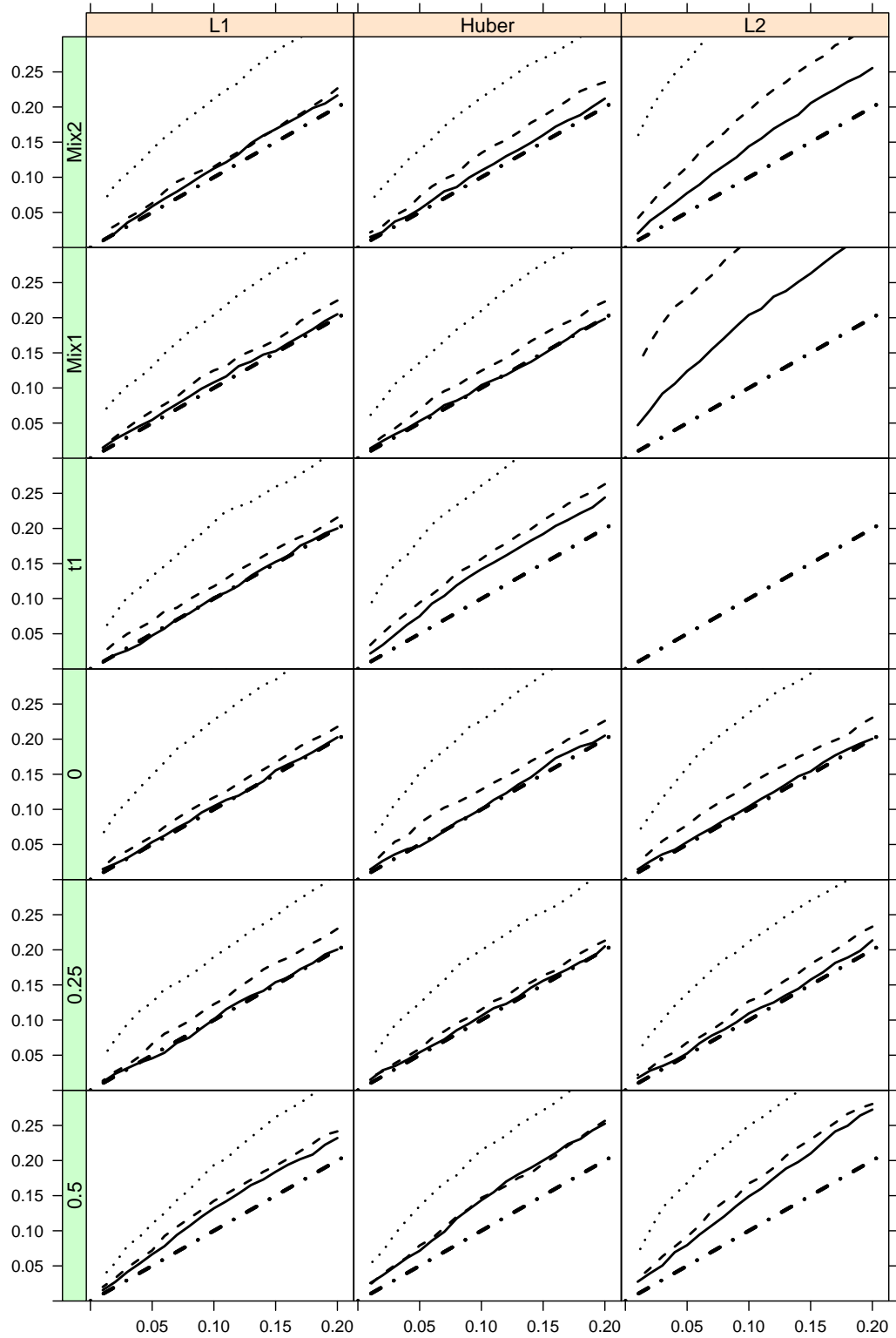


Figure 31: SPC for different procedures with FLT estimator with $\Lambda_m = 4$ under H_0 , different distributions of errors in each panel, $\gamma = 0.25$.
 $m : 80$ - dotted, 200 - dashed, 400 - solid.

2.2 Figure 6.16

Next four figures present DRL (on the left) and DPC (on the right) of the procedures for different distributions, $k^* = 200$, $\gamma = 0.25$. First two figures are for QS estimator, last two for the FLT one. We consider alternatives of change in both or just one component.

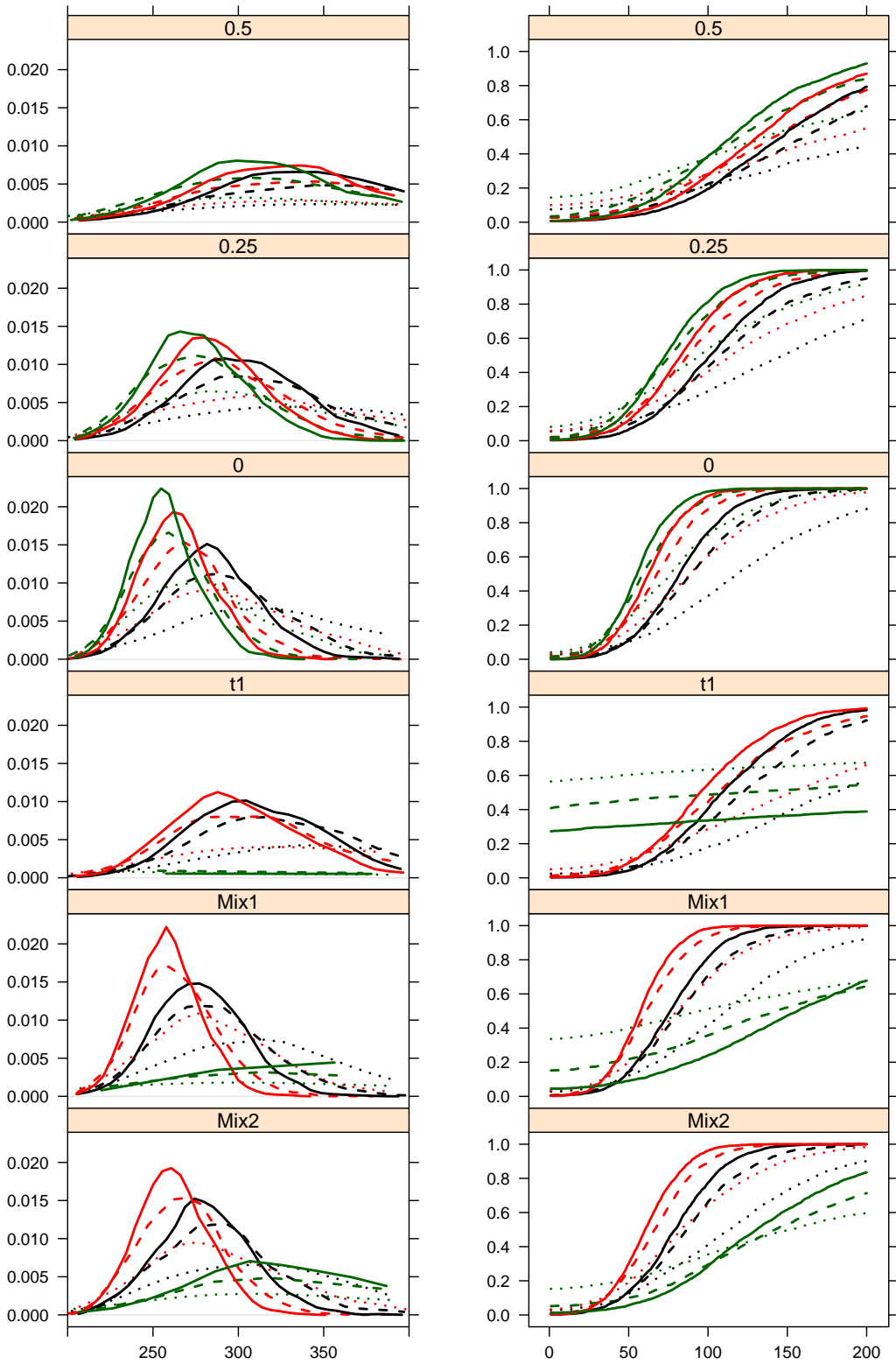


Figure 32: DRL (on the left) and DPC (on the right) of the procedures for different distributions, $k^* = 200$, $\gamma = 0.25$, $\delta_m \boldsymbol{\theta} = (1, 1)^T$, adaptive QS estimator.
 Procedure: Huber - black, L_1 - red, L_2 - green; m : 80 - dotted, 200 - dashed, 400 - solid.

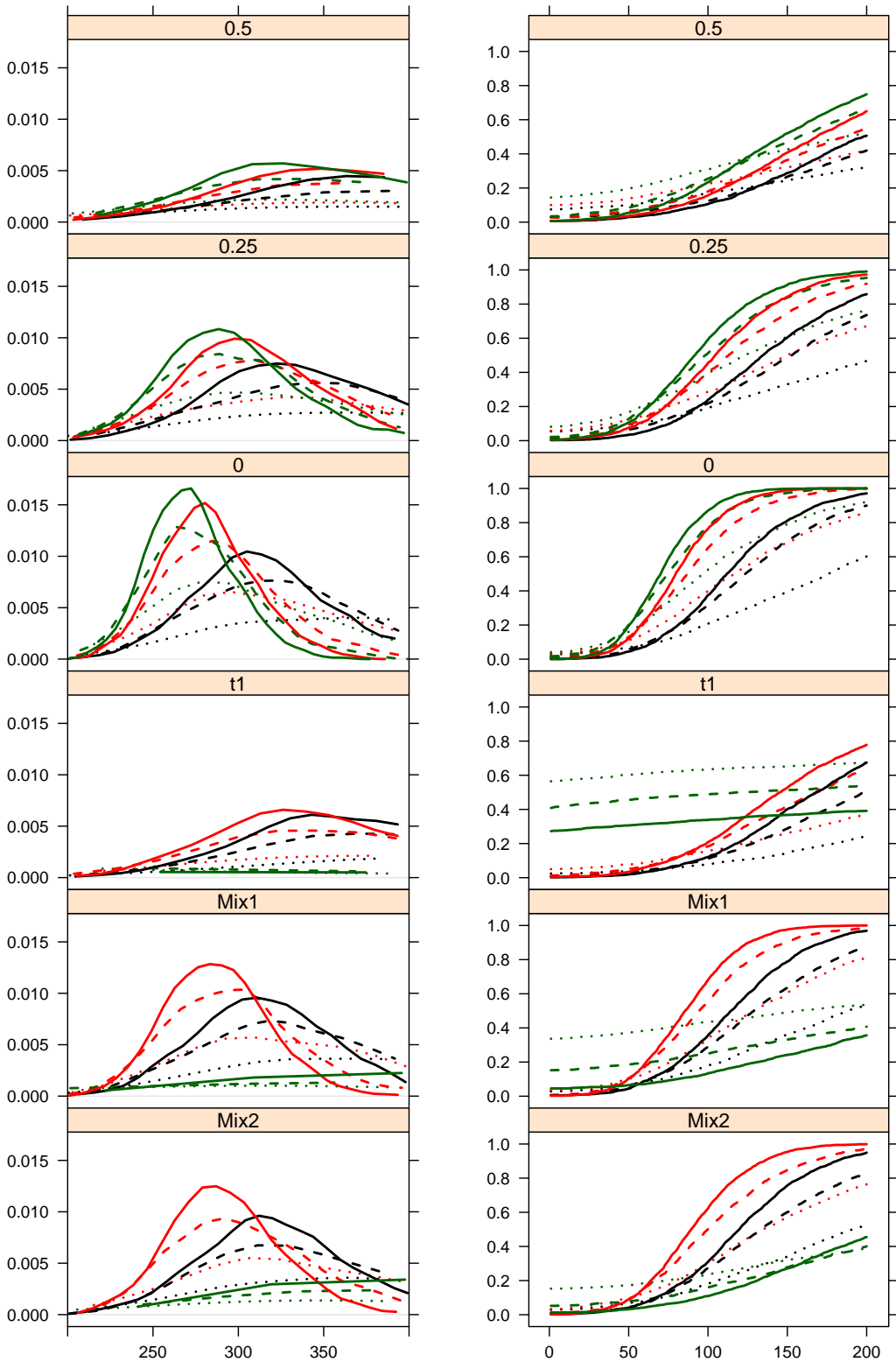


Figure 33: DRL (on the left) and DPC (on the right) of the procedures for different distributions, $k^* = 200$, $\gamma = 0.25$, $\delta_m \theta = (1, 0)^T$, adaptive QS estimator.
 Procedure: Huber - black, L_1 - red, L_2 - green; m : 80 - dotted, 200 - dashed, 400 - solid.

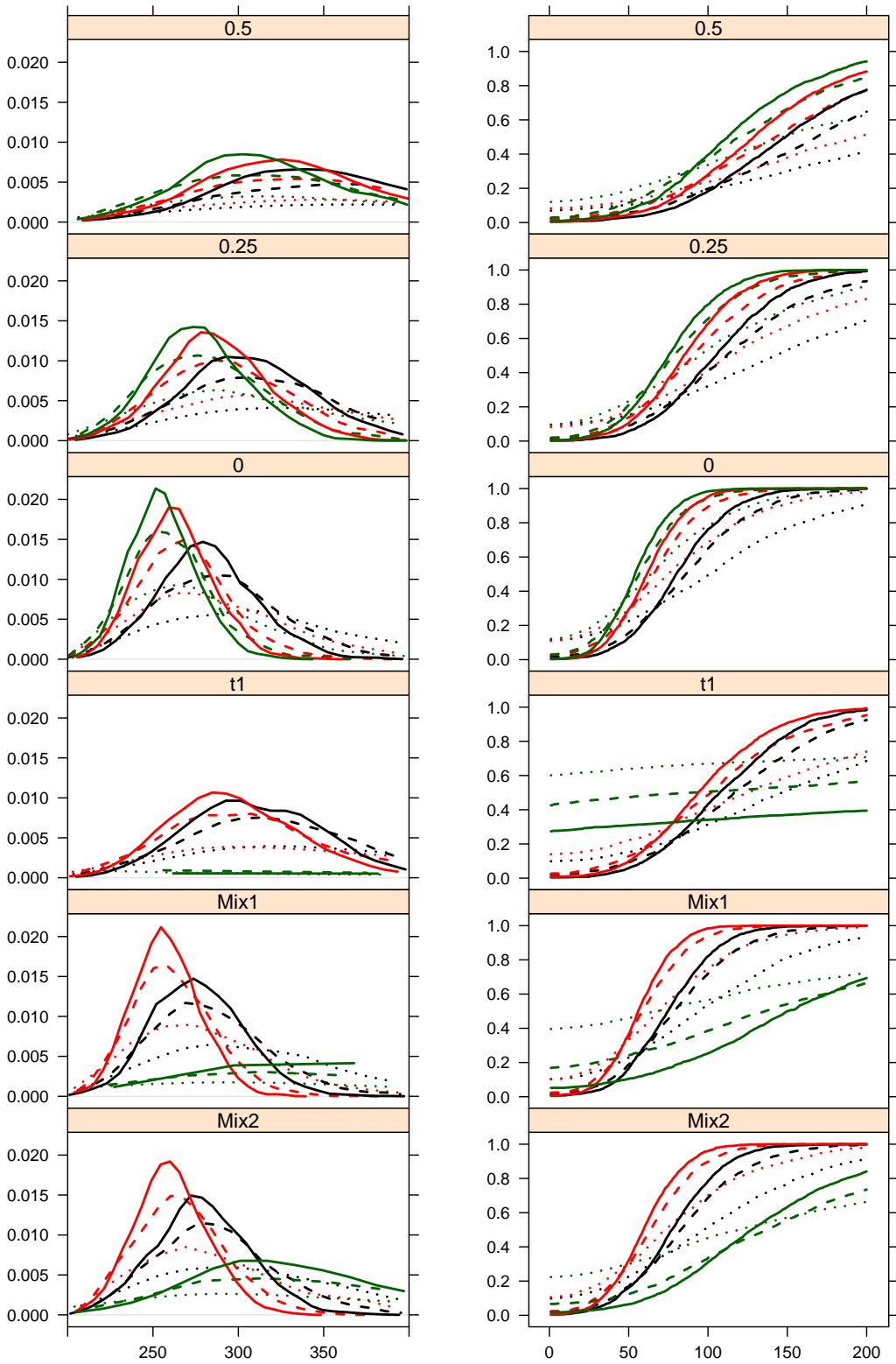


Figure 34: DRL (on the left) and DPC (on the right) of the procedures for different distributions, $k^* = 200$, $\gamma = 0.25$, $\delta_m \boldsymbol{\theta} = (1, 1)^T$, fixed FLT estimator.

Procedure: Huber - black, L_1 - red, L_2 - green; m : 80 - dotted, 200 - dashed, 400 - solid.

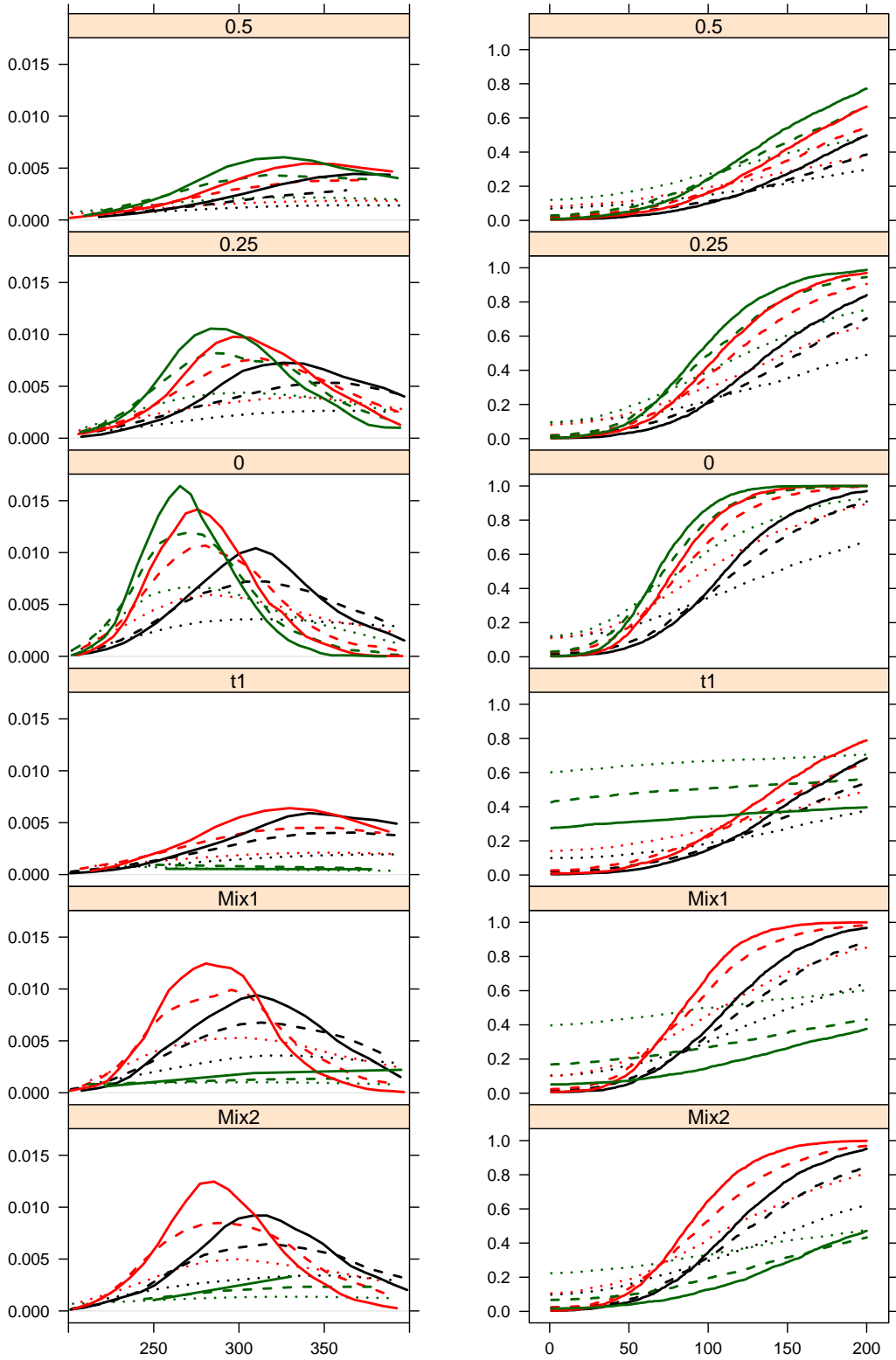


Figure 35: DRL (on the left) and DPC (on the right) of the procedures for different distributions, $k^* = 200$, $\gamma = 0.25$, $\delta_m \boldsymbol{\theta} = (1, 0)^T$, fixed FLT estimator.

Procedure: Huber - black, L_1 - red, L_2 - green; m : 80 - dotted, 200 - dashed, 400 - solid.

3 Capital Asset Pricing Model

In this section we compare figures obtained with adaptive Quadratic Spectral estimator with those using the FLT one with fixed $\Lambda_m = 4$. We start with the null hypothesis (i.e. Figure 6.17 of the thesis), which is followed by alternatives, where also different kinds are presented.

3.1 Figure 6.17

SPC for different procedures under H0, with adaptive QS estimator or fixed FLT one, different distributions of errors in each panel, $\gamma = 0.25$.

C_H0_AdP_12_2000

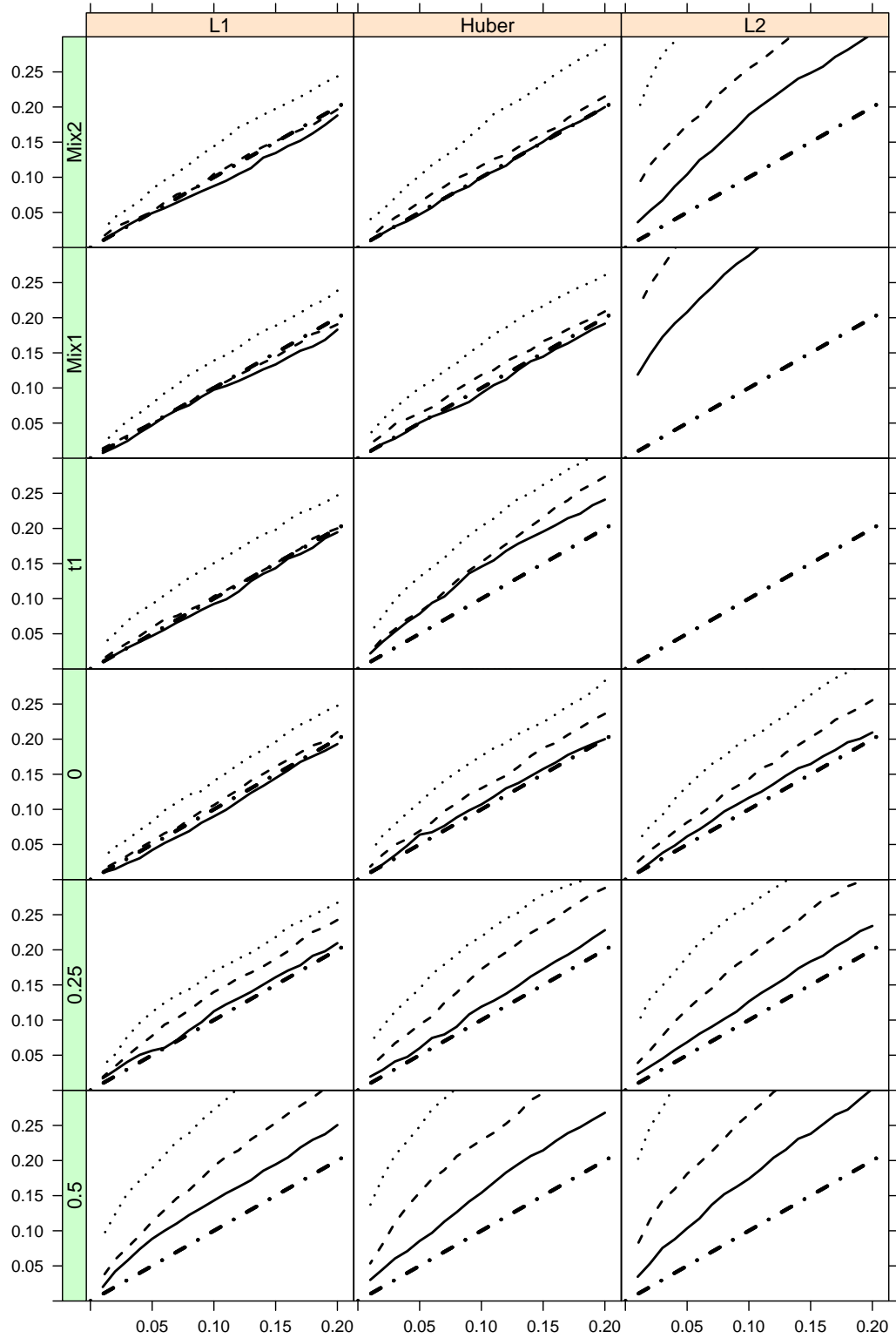


Figure 36: SPC for different procedures with adaptive QS estimator under H_0 , different distribution of errors in each panel, $\gamma = 0.25$.
 $m : 80$ - dotted, 200 - dashed, 400 - solid.

C_H0_FLT_12_2000

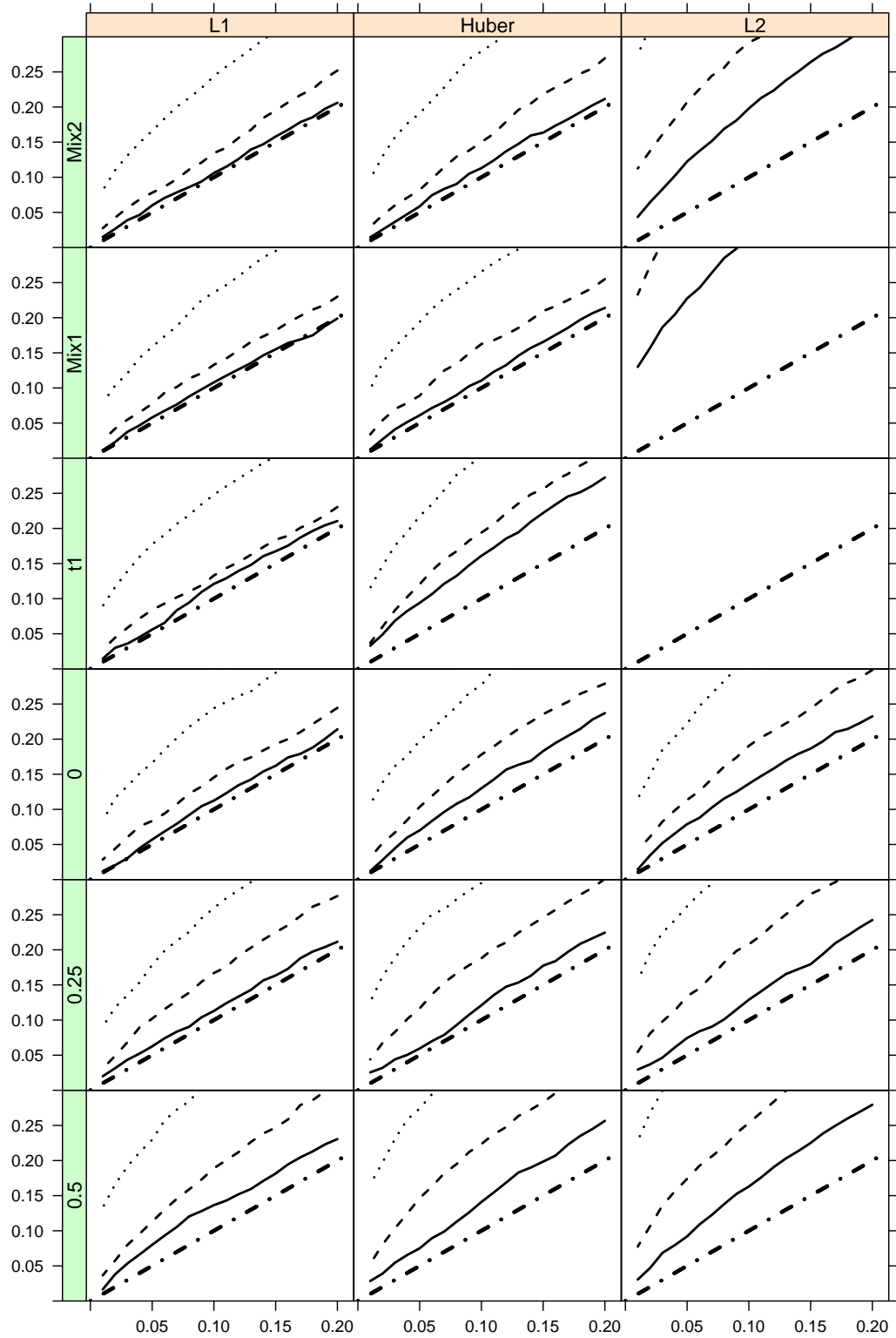


Figure 37: SPC for different procedures with FLT estimator under H_0 , different distribution of errors in each panel, $\gamma = 0.25$.
 $m : 80$ - dotted, 200 - dashed, 400 - solid.

3.2 Figure 6.18

Following figures present DRL (on the left) and DPC (on the right) of the procedures for different distributions, $k^* = 200$, $\gamma = 0.25$. Next four use adaptive QS kernel LRV estimator. Considered alternatives are changes in both components of portfolio betas $\delta_m\beta_1 = (1, 1)^T$, $\alpha_1 = \mathbf{0}$, the previous one with change in intercept also $\delta_m\beta_1 = (1, 1)^T$, $\delta_m\alpha_1 = (1, 1)^T$, change in just one component of portfolio betas $\delta_m\beta_1 = (1, 0)^T$, $\alpha_1 = \mathbf{0}$ and change in intercept only $\delta_m\beta_1 = \mathbf{0}$, $\delta_m\alpha_1 = (1, 1)^T$.

Last two figures use fixed FLT estimator, where we consider change in both components of portfolio betas $\delta_m\beta_1 = (1, 1)^T$, $\alpha_1 = \mathbf{0}$ and the previous one with change in intercept also $\delta_m\beta_1 = (1, 1)^T$, $\delta_m\alpha_1 = (1, 1)^T$.

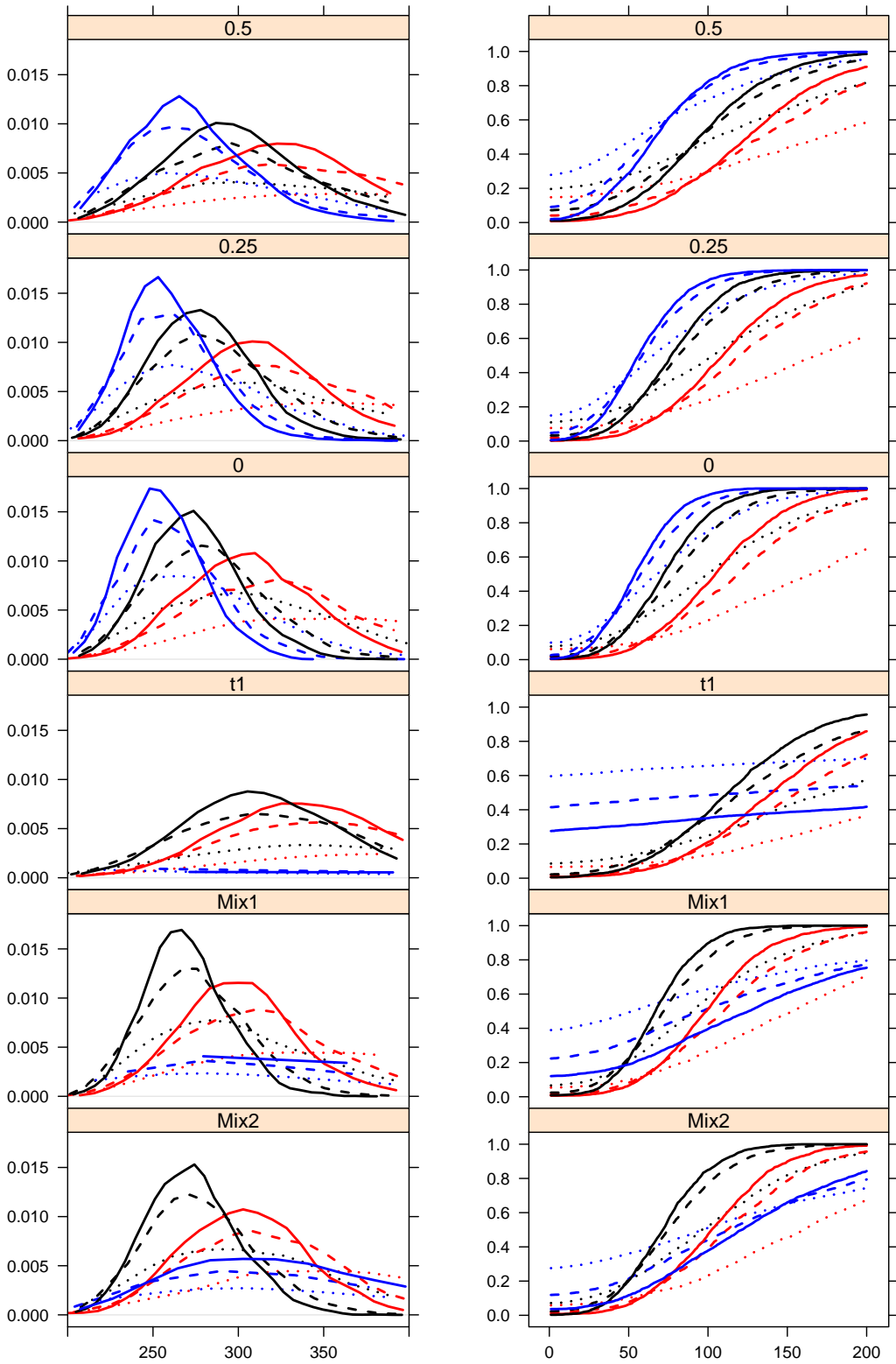


Figure 38: DRL on the left and DPC on the right, adaptive QS kernel, $\delta_m \beta_1 = (1, 1)^T$, $\alpha_1 = \mathbf{0}$.

Procedure: Huber - black, L_1 - red, L_2 - blue; $m : 80$ - dotted, 200 - dashed, 400 - solid.

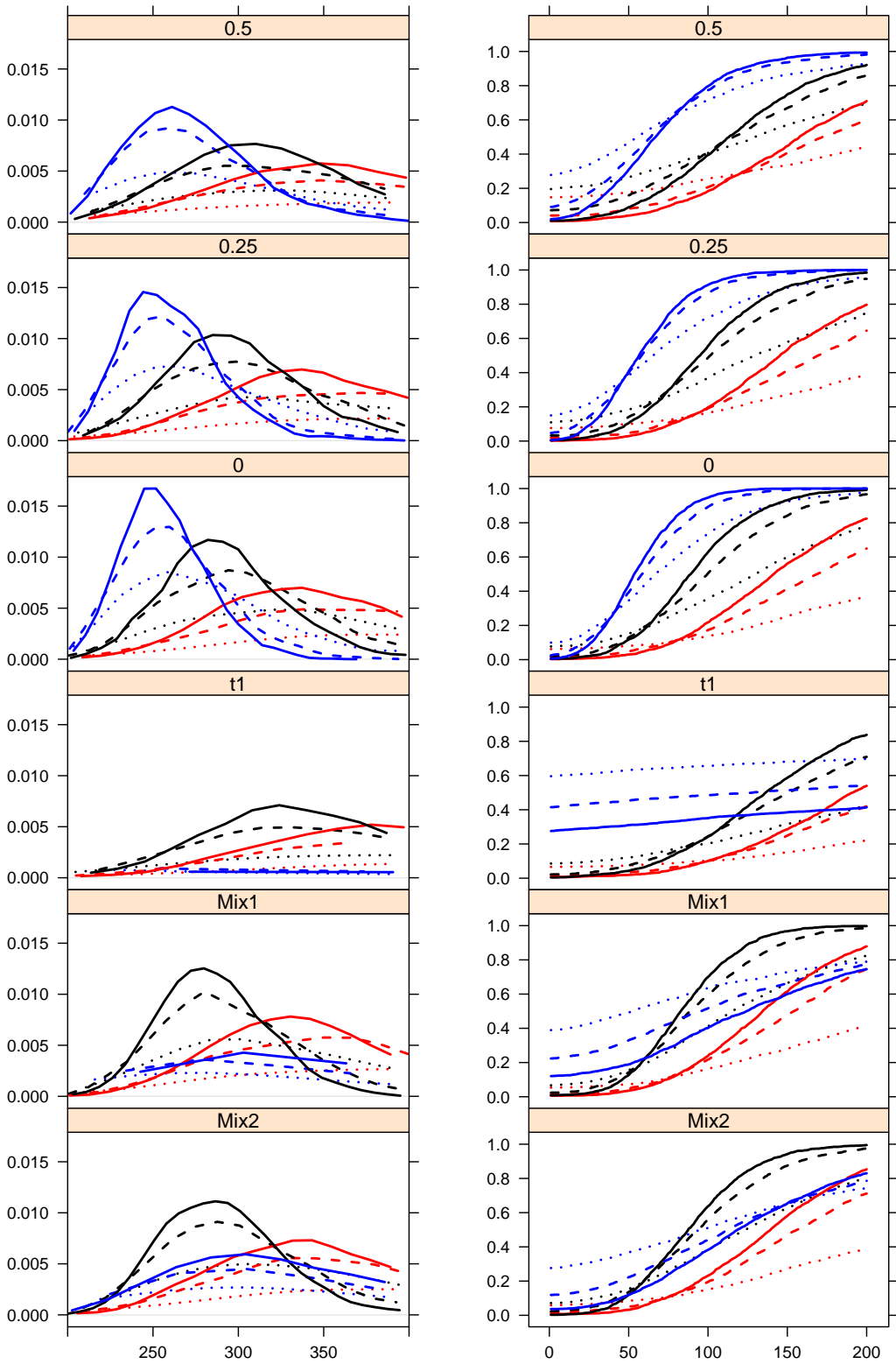


Figure 39: DRL on the left and DPC on the right, adaptive QS kernel, $\delta_m \beta_1 = (1, 1)^T$, $\delta_m \alpha_1 = (1, 1)^T$.

Procedure: Huber - black, L_1 - red, L_2 - blue; $m : 80$ - dotted, 200 - dashed, 400 - solid.

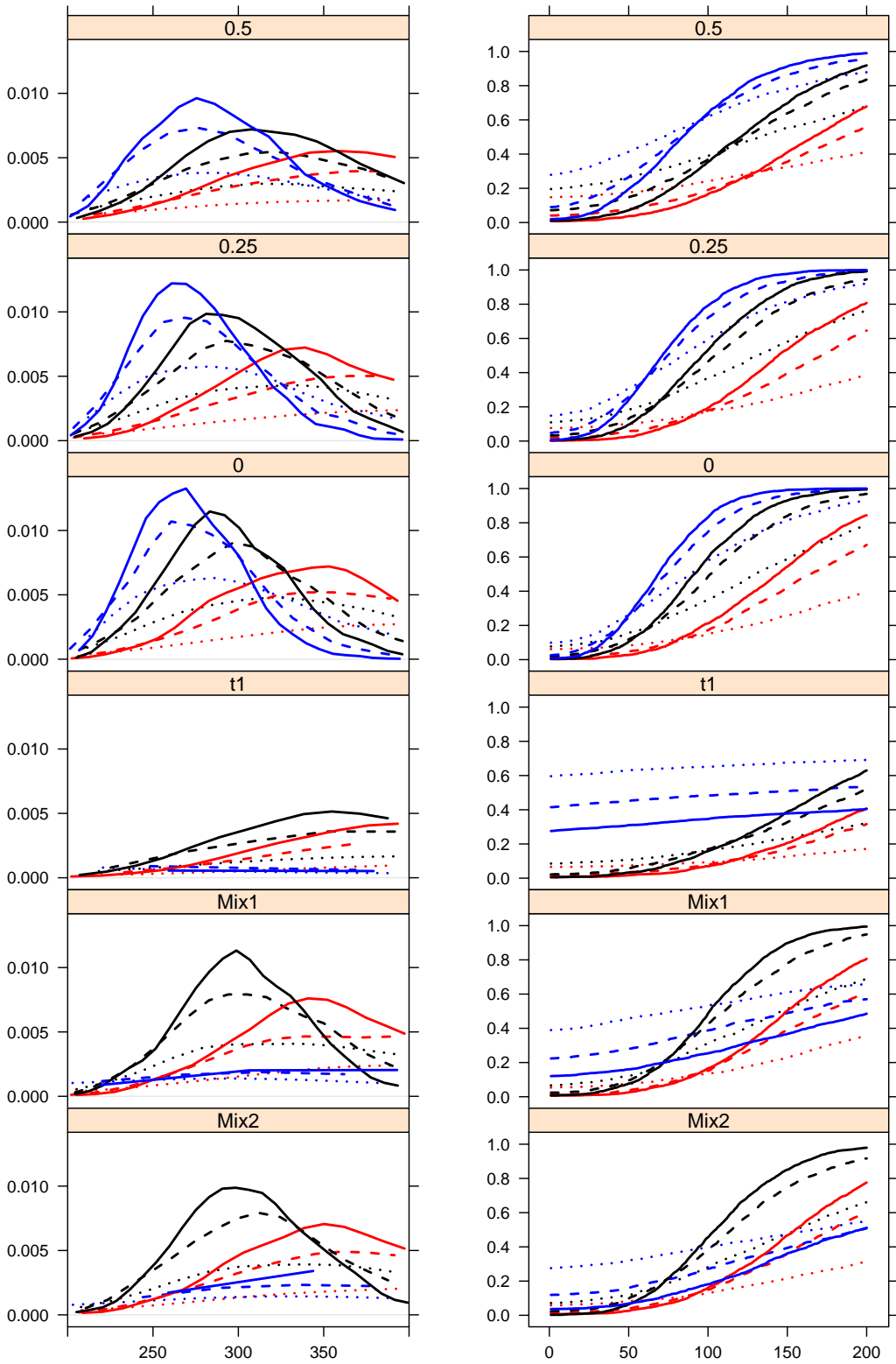


Figure 40: DRL on the left and DPC on the right, adaptive QS kernel, $\delta_m \beta_1 = (1, 0)^T$, $\alpha_1 = \mathbf{0}$.

Procedure: Huber - black, L_1 - red, L_2 - blue; m : 80 - dotted, 200 - dashed, 400 - solid.

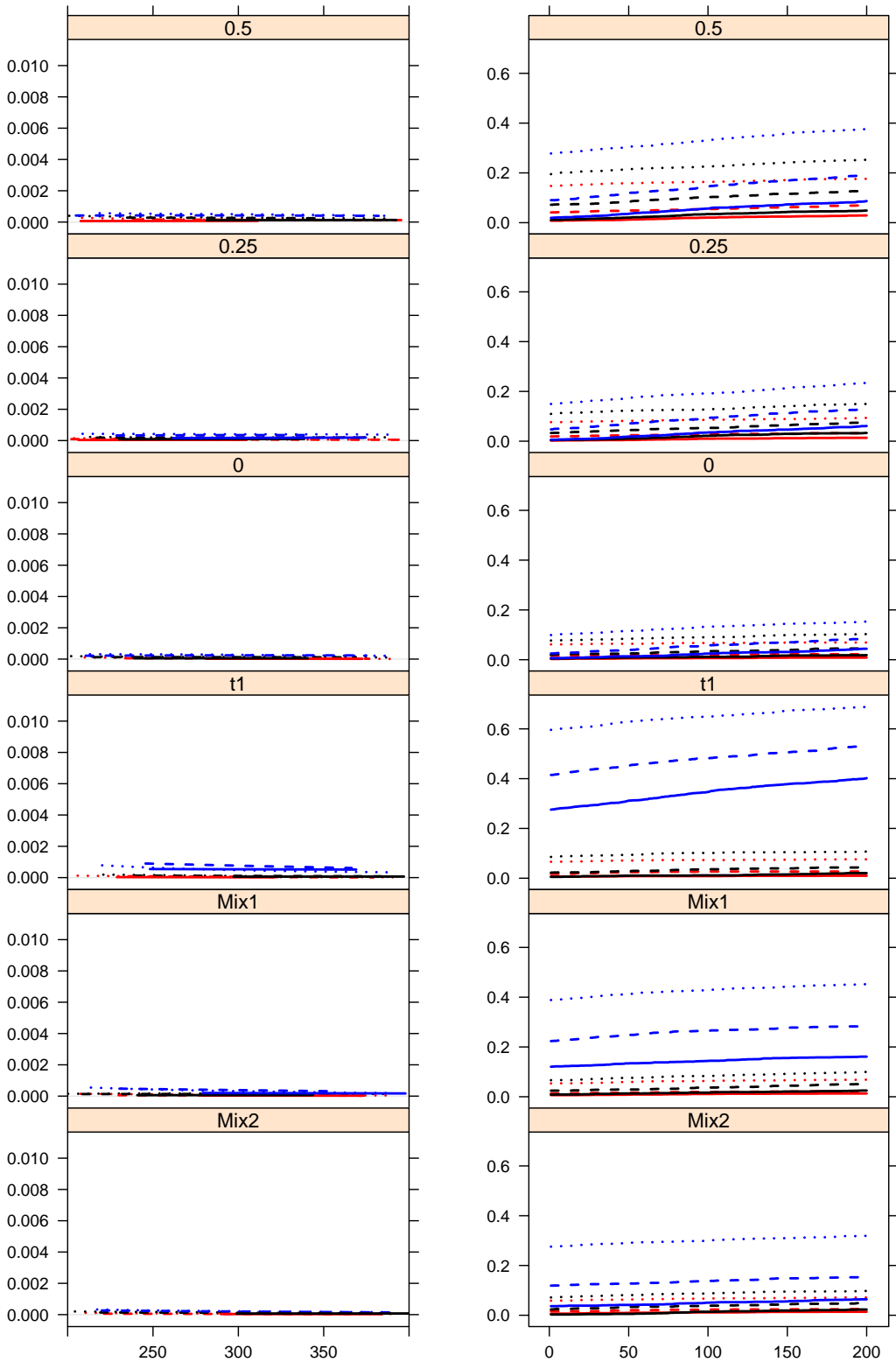


Figure 41: DRL on the left and DPC on the right, adaptive QS kernel, $\delta_m \beta_1 = \mathbf{0}$, $\alpha_1 = (1, 1)^T$.

Procedure: Huber - black, L_1 - red, L_2 - blue; m : 80 - dotted, 200 - dashed, 400 - solid.

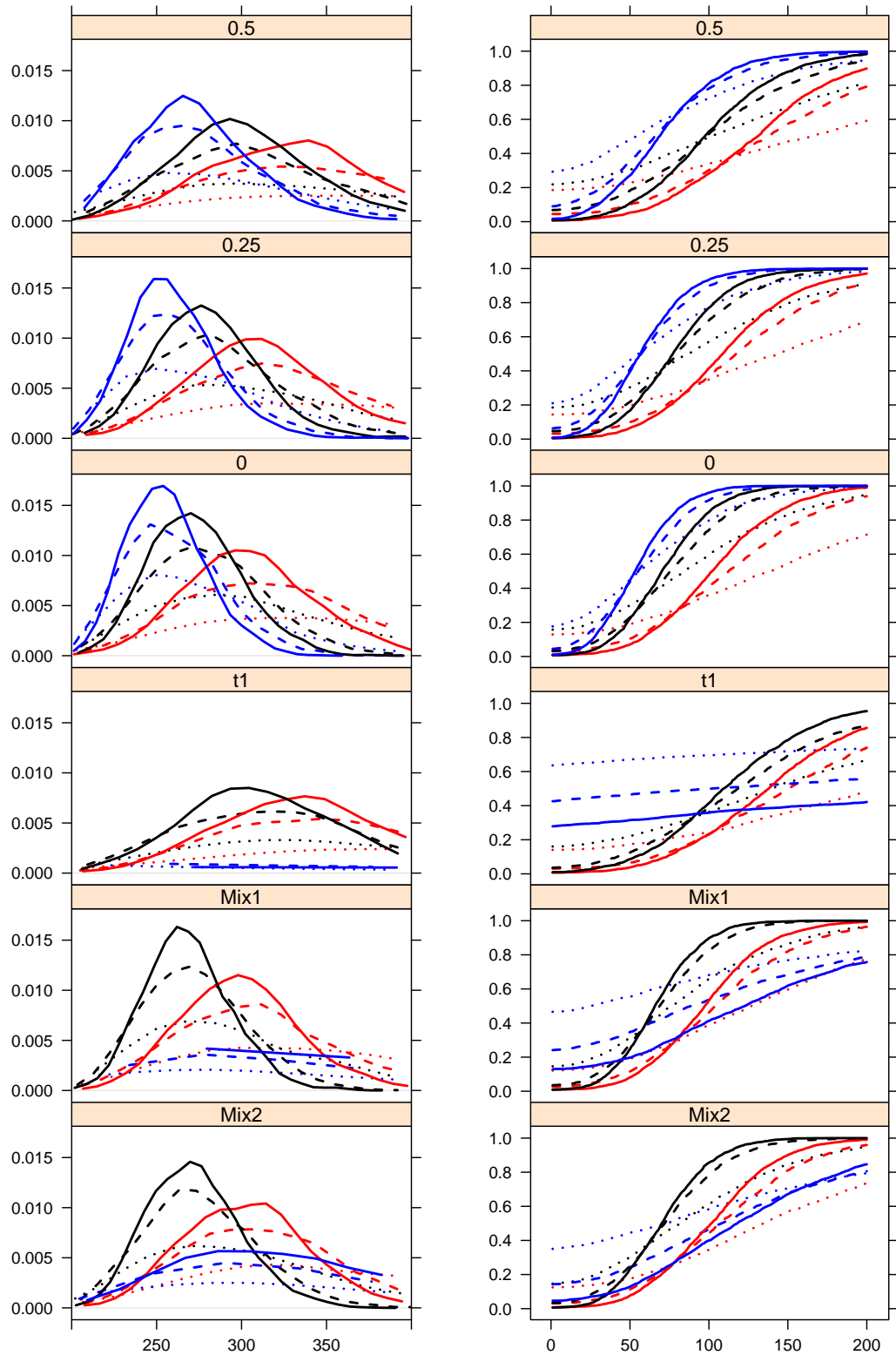


Figure 42: DRL on the left and DPC on the right, FLT kernel, $\delta_m \beta_1 = (1, 1)^T$, $\alpha_1 = \mathbf{0}$. Procedure: Huber - black, L_1 - red, L_2 - blue; m : 80 - dotted, 200 - dashed, 400 - solid.

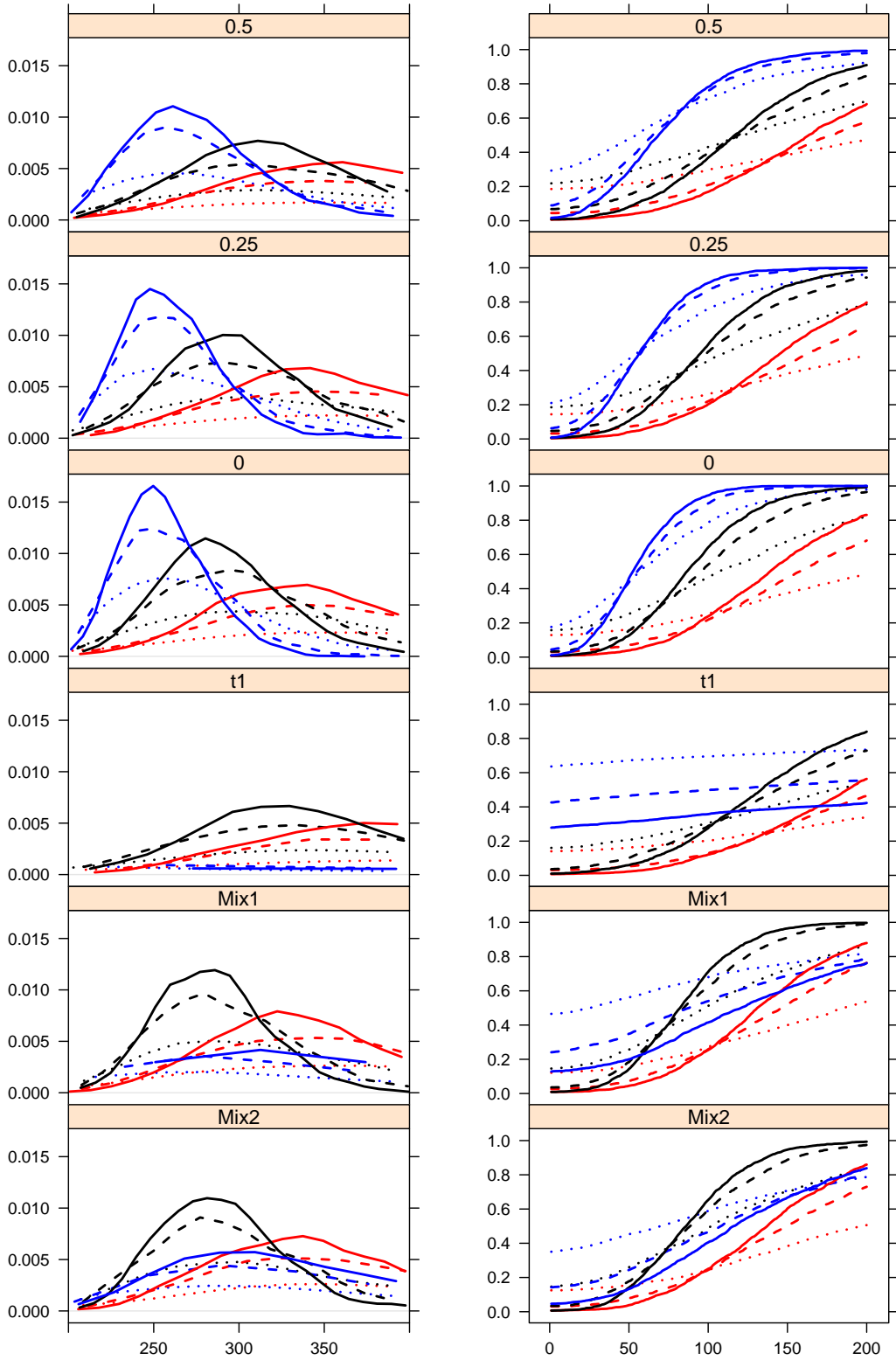


Figure 43: DRL on the left and DPC on the right, FLT kernel, $\delta_m \beta_1 = (1, 1)^T$, $\delta_m \alpha_1 = (1, 1)^T$.

Procedure: Huber - black, L_1 - red, L_2 - blue; m : 80 - dotted, 200 - dashed, 400 - solid.